

**EXPLORING THE CAPABILITIES
OF THE HOUGHTON COLLEGE
CYCLOTRON**

By

Nicholas A. Fuller

A thesis submitted in partial fulfillment of the
requirements for the degree of

Bachelor of Science

Houghton College

August 2013

Signature of Author.....

Department of Physics
August 5, 2013

.....

Dr. Mark Yuly
Professor of Physics
Research Supervisor

.....

Dr. Brandon Hoffman
Associate Professor of Physics

**EXPLORING THE
CAPABILITIES OF THE
HOUGHTON COLLEGE
CYCLOTRON**

By

Nicholas A. Fuller

Submitted to the Department of Physics
on August 5, 2013 in partial fulfillment of the
requirement for the degree of
Bachelor of Science

Abstract

The Houghton College Cyclotron is currently capable of accelerating protons to 317 keV, and with an improved magnet power supply and cooling should achieve 400 keV. Low pressure hydrogen or helium gas is introduced into the vacuum chamber where a filament, through electron collisions, ionizes the gas. The ions are accelerated in a spiral path of 72 mm maximum radius by an alternating RF electric field in a constant magnetic field of up to 1.2 T. The cyclotron's performance has been characterized for varying gas pressure, filament voltage, orbit radii, and “dee” voltage. In the near future, low energy nuclear reactions such as $D(d,n)^3\text{He}$ and $D(^3\text{He},p)^4\text{He}$, as well as high-yield (p,γ) resonances like $^{19}\text{F}(p,\gamma)^{16}\text{O}$ and $^{31}\text{P}(p,\gamma)^{32}\text{S}$ may be studied.

Thesis Supervisor: Dr. Mark Yuly

Title: Professor of Physics

TABLE OF CONTENTS

Chapter 1	6
1.1 History and Motivation	6
1.2 The Cyclotron	9
1.2.1 Acceleration Method.....	10
1.2.2 Development of the Cyclotron.....	11
1.2.3 History of Miniature Cyclotrons.....	12
1.2.4 The Houghton College Cyclotron.....	14
Chapter 2	16
2.1 The Resonance Principle	16
2.1.1 Fundamental Frequency.....	16
2.1.2 Harmonics.....	18
2.2 Tuned LC Circuits	19
2.3 Relativistic Considerations	23
2.4 Determining Ion Energy	24
2.5 Path Length	25
2.6 Beam Focusing	26
2.6.1 Electrostatic Focusing.....	26
2.6.2 Magnetic Focusing.....	28
Chapter 3	32
3.1 Overview	32
3.2 Electromagnet	33
3.3 Chamber	34
3.4 Vacuum and Gas System	35
3.5 Filament	37
3.6 RF System	37
3.6.1 RF Tuning	41
3.7 Beam Collector	43
3.8 Control System	44
Chapter 4	46

4.1	Magnet Scans	46
4.2	Effect of Filament Bias Voltage	48
4.3	Effect of Dee Voltage	49
4.4	Pressure Effects.....	51
4.5	Beam Current at Varying Collector Radii	52
4.6	Increasing Frequency	54
4.7	Effect of Secondary Electrons	55
Chapter 5	57
Appendix	60

TABLE OF FIGURES

Figure 1. Schematic of a Van de Graaff accelerator.....	7
Figure 2. Diagram of a two-stage tandem accelerator.....	8
Figure 3. Diagram of a linear accelerator.....	9
Figure 4. A particle's trajectory within a cyclotron.....	10
Figure 5. Photograph of the Livingston and Lawrence's 1.2 MeV cyclotron.....	11
Figure 7. Force diagram for a charged particle moving in a magnetic field.....	16
Figure 8. Harmonic frequencies of a cyclotron.....	19
Figure 9. A coupled LC circuit.....	19
Figure 10. Graph of ion energies as a function of magnetic field.....	25
Figure 11. Diagram depicting electrostatic focusing.....	27
Figure 12. The focusing effect of a non-uniform magnetic field.....	28
Figure 13. The cylindrical coordinate system used.....	29
Figure 14. Photograph of the Houghton College cyclotron.....	32
Figure 15. Plot of magnetic field strength as a function of current.....	33
Figure 16. Photograph of the inside of the chamber.....	35
Figure 17. Schematic of the vacuum and gas system.....	36
Figure 18. The Houghton College cyclotron RF system.....	38
Figure 19. The previous LC circuit.....	39
Figure 20. The new LC circuit.....	40
Figure 21. VIA Bravo Graph of SWR versus frequency.....	41
Figure 22. Graph of SWR as a function of frequency obtained by hand.....	42
Figure 23. Voltage calibration for the f=5.8 MHz tune.....	43
Figure 21. Beam collector circuit diagram.....	44
Figure 22. Block diagram of the control system.....	45
Figure 26. Plot of a magnet scan at f=3.68 MHz.....	47
Figure 27. The highest beam current recorded to date.....	47
Figure 28. Effect of filament bias on beam current.....	48
Figure 29. Effect dee voltage bias on beam current.....	50
Figure 30. Effect of gas pressure on beam current.....	51
Figure 31. Full scans at different current collector radii.....	52
Figure 29. Beam current as a function of collector radius.....	53
Figure 30. Beam current at 12.13 MHz.....	54
Figure 34. The effect of secondary electrons on measured currents.....	56
Figure 35. Cross section plot of the $^{19}\text{F}(p, \gamma)^{16}\text{O}$ resonance.....	58
Figure 36. Schematic of an experiment measuring the $^3\text{H}(^3\text{He}, p)^4\text{He}$ resonance.....	59

Chapter 1

INTRODUCTION

1.1 History and Motivation

In his 1927 annual address to the Royal Society of London [1], Sir Ernest Rutherford explained the then recent development of a series of high voltage vacuum tubes capable of accelerating ions across a 900,000 V potential. He noted that although this was no small feat, physicists had yet to produce a beam of particles of energy greater than those naturally produced in radioactive decay. In fact, the α particle released in the decay of “Radium C” has an energy of 7.6 MeV- which would require potentials of 3.8 million volts to artificially produce. Rutherford noted that higher energy particles could be used to probe atomic nuclei and that artificially production would produce higher currents and finer control over the energies than could be offered by using radioactive decay products. Even so, he realized there were still large obstacles to overcome before such machines could be built.

Fortunately, Rutherford did not have to wait very long for these developments. In 1931, R.J. Van de Graff presented his accelerator at the Schenectady meeting of the American Physical Society [2]. His accelerator, capable of generating 1.5 million volt potentials, was a simple electrostatic generator made of inexpensive parts as shown in Figure 1. Charges were added to an insulating belt via a charged comb and then traveled on the belt. These charges were then transferred onto the spherical high voltage terminal by another conductive comb. As charge was added to the terminal, electrical potential built up between the sphere and ground. This potential was then be used to accelerate charged particles.

Although one of the earliest accelerator designs, modern Van de Graff accelerators are still used today. By controlling the amount of charge delivered to the conducting sphere, physicists are able to precisely

control the energy of the accelerated particles. Even better, the emerging particles are nearly monoenergetic, which is ideal for experiments that demand precise energy resolution.

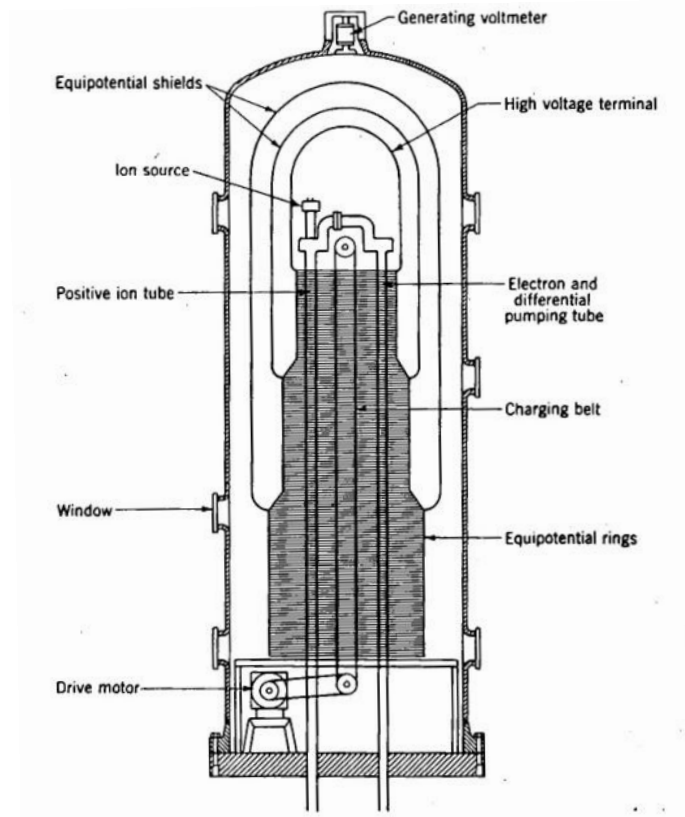


Figure 1. A schematic of a Van de Graaff accelerator. A silk belt is “sprayed” with charges that are collected by the spherical electrode, causing a large build up of potential that can be used to accelerate ions. Figure taken from Ref.[3].

Many electrostatic accelerators, including the Van de Graff, require large potentials to produce high energy particles for physics experiments. Although this is not a theoretical issue, in practice there are limitations to the potentials achievable. This was the motivation behind the development of the tandem Van de Graff accelerator [3].

By changing the charge of the ions being accelerated, a tandem accelerator can use the same high potential twice to accelerate the beam, as shown in Figure 2. This effectively doubles the beam energy for a given terminal voltage.

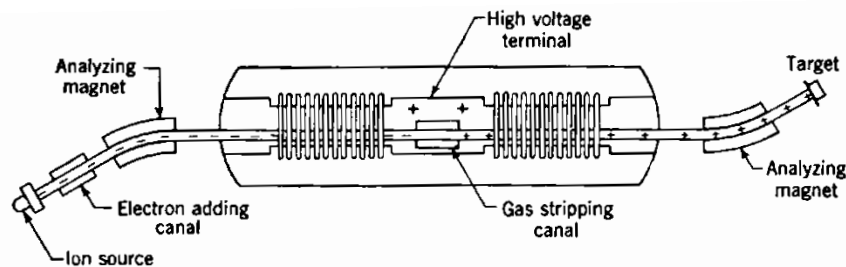


Figure 2. A diagram of a two-stage tandem accelerator. In this configuration, electrons are first added to the particles to be accelerated. Once within the positive electrode the atoms are stripped of their electrons. The now positive ions are repelled away from the positive terminal. In this way, the same potential is used to accelerate the particles twice. Figure taken from Ref.[4].

Rather than change the charge of the ions being accelerated, the polarity of a series of electrodes could be alternated in order to accelerate the same ion numerous times. This is the idea behind the design of linear accelerators [5]. As the name might imply, a linear accelerator uses a linear series of electrodes whose voltages oscillate at a high frequency. As shown in Figure 3, a particle will be accelerated by the potential in the gap between electrodes. The particle then drifts into a channel passing through conducting the electrode, during which time the voltage is switched so that when the particle emerges from the other side it is accelerated across the next gap. Since the potential is switched while the particle is inside the conductor where there is no electric field, the particle is not affected. By making each electrode longer, the drift time inside each electrode can be made constant so a single frequency can be applied to all the electrodes.

One advantage of the linear accelerator is that the maximum voltage needed for a given energy is just the voltage between the electrodes. In an electrostatic accelerator a voltage equal to the maximum

particle energy is required. Indeed, one could always increase the maximum energy attained by lengthening the linear accelerator. So instead of voltage limitations, one runs into the issue of size constraints.

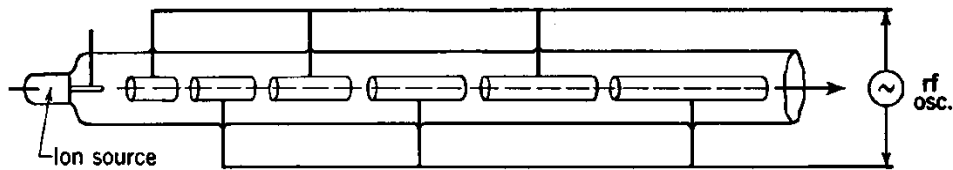


Figure 3. Diagram of a linear accelerator. A radio frequency is applied to the electrodes in such a way that voltage between gaps will be switched when ions are within an electrode. In this way a linear accelerator can use lower voltages to produce high energy particles over a long accelerator. Figure taken from Ref. [5].

Without a solution to the issues of voltage and size limitations, it seemed that accelerators would be limited by sparking or by sheer size. Fortunately, an accelerator capable of using relatively low accelerating potentials while fitting into an average sized laboratory was developed, the cyclotron.

1.2 The Cyclotron

In his Nobel lecture [6], E.O. Lawrence discussed how he developed the idea of magnetic resonance as a potential solution to the issues encountered by early accelerators. After reading about the recent development of the linear accelerator [7] and its method of multiple accelerations, he began to wonder if the same two electrodes might be used repeatedly to accelerate particles. By using a uniform magnetic field, Lawrence found that a particle could be accelerated in circular paths of increasing radii while using the same low-voltage electrodes repeatedly. In this way one might overcome the two primary downfalls of other accelerators: voltage and size constraints.

1.2.1 Acceleration Method

The cyclotron accelerates particles as shown in Figure 4. The particles then drift in the hollow “dee”, uninfluenced by electric fields since they are inside a conductor. A magnetic field perpendicular to the particle’s path causes the particle to experience a force toward the center of the chamber, constraining the particles to a circular orbit. While the particle is drifting in this circular path within the electrode, the potential is reversed on the dees so that as the particle emerges into the acceleration gap it is accelerated again.

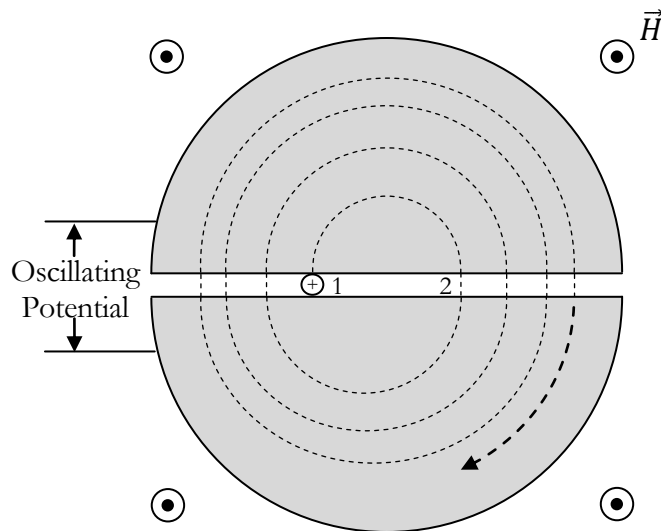


Figure 4. A particle’s trajectory within a cyclotron. A neutral atom is ionized at point 1 via a filament. A voltage applied between the dees accelerates the particle into the upper dee. A uniform magnetic field (H) orthogonal to the particles path generates a centripetal force that enables the particle to orbit in a clockwise fashion. While within the upper dee, the voltage between the dees switches polarity so that as the particle arrives at 2 it is accelerated again. The process is repeated until the particle reaches the edge of the chamber.

Hence, by oscillating the potential between the electrodes at the proper frequency, the particles will reach the gap at the proper time to be accelerated repeatedly, increasing the radius of the orbit until particles reach the edge of the chamber. At that point, the energy of the particles will be much greater

than the potential used to accelerate them. Since (for non-relativistic energies) the period of the particles orbit is constant regardless of the orbital radius, the driving frequency can be held constant.

1.2.2 *Development of the Cyclotron*

In 1931, M.S. Livingston wrote his doctoral thesis [8] on the first magnetic resonance accelerator, or cyclotron, based on the concept of magnetic resonance developed by E.O. Lawrence. Designed primarily as a proof of concept, this cyclotron produced 80 keV hydrogen ions using a 2000 V oscillating dee potential and a 1.3 T magnetic field. He was able to observe 0.3 nA of beam current using a current collector at a radius of 4.5 cm, showing the feasibility of using magnetic resonance as an acceleration method.

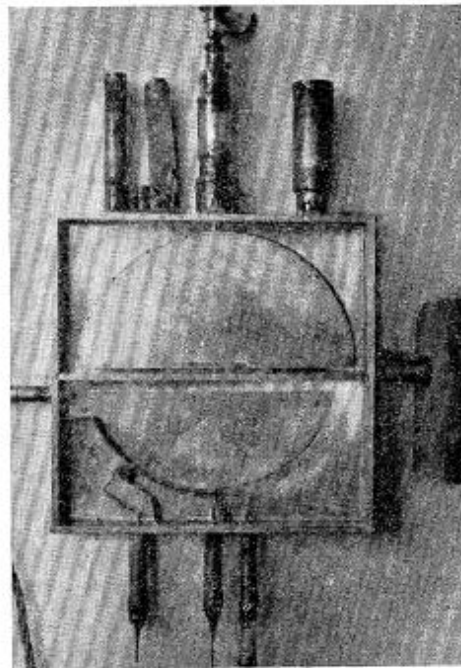


Figure 5. Photograph of the Livingston and Lawrence's 1.2 MeV cyclotron. The electrodes were made of brass with cavities allowing particles to orbit inside, free of electric fields. The grounded dee is smaller to allow for easier beam extraction. Figure taken from Ref. [8].

Once the concept of the cyclotron was shown to be feasible, Livingston and Lawrence set out to design a cyclotron capable of producing higher energies. Figure 5 shows an accelerator capable of producing 1.2 MeV protons [9] and was the second cyclotron built by Lawrence and Livingston. This was achieved by increasing the chamber size to 24 cm in diameter and using a 1.4T electromagnet. In order to simplify the RF circuit, only one dee was connected to the oscillating voltage while the other was simply grounded.

Just four years later Lawrence had developed a 23 inch cyclotron [10] capable of producing 6.3 MeV deuterons at several microamperes of current and 11 MeV α -particles at a few tenths of a microampere. In addition to a beam extractor, a beryllium target within the chamber could be used to produce neutrons. Other target materials were bombarded with 5 MeV deuterons to produce radioactive isotopes of many elements. In 1939, Lawrence and his team at Berkley had successfully tested the 60 inch cyclotron [11]. This machine was capable of producing 8 MeV protons, 16 MeV deuterons and 38 MeV α -particles.

At this point, the cyclotron was nearing the maximum energy obtainable. In 1937, it was noted [12] that relativistic effects would ruin the fixed-frequency resonance condition. Although the magnetic field could be increased with radius to remain in resonance, such a field would defocus the beam and greatly reduce beam current.

One way to overcome this limitation is to create a frequency modulated cyclotron [13], more commonly known as a synchrocyclotron. Tested in 1948, it was shown that decreasing the frequency once particles reached high speeds could account for relativistic effects. This allowed higher energies to be obtained without defocusing the particle beam.

1.2.3 History of Miniature Cyclotrons

As will be shown in the next chapter, a cyclotron's energy is limited by the maximum radius and magnetic field strength attainable. Thus, higher energies could be made by constructing larger chambers and electromagnets. However, for some applications it is desirable to have a smaller

machine of comparable size to Livingston's original cyclotron. In the past as well as in recent years, there has been an interest in the use of these small cyclotrons for experiments [14-22].

In the spring of 1948, four seniors at El Cerrito high school designed and began building a cyclotron [14], becoming the first high school students to do so. With a dee diameter of 6 inches, the El Cerrito cyclotron produced a 7 μ A proton beam at energies up to 1 MeV.

The first cyclotron built by undergraduates was undertaken by students of Iowa State University beginning in 1954 and produced beam in the spring of 1957. Using a 1.7 T electromagnet and a 10 inch diameter chamber, the ISU cyclotron was capable of producing 1.5 MeV protons for nuclear physics experiments [15]. Another example of an undergraduate cyclotron [16] was built by Jeffery C. Smith of Knox College. Starting as a junior, Smith constructed a 1.5 MeV fixed-frequency cyclotron that was nearing completion at the time of his graduation in 2001. A third undergraduate cyclotron [17] was built by Leslie Dewan at MIT and was capable of accelerating protons to 2 MeV for nuclear physics experiments- particularly the ${}^7\text{Li}(p, n){}^7\text{Be}$ reaction.

With the goal of creating a cyclotron much like the original built by Livingston, Fred Neil built a "garage cyclotron" in 1994 [18]. Using a two dee design and a hand-turned 0.78 T electromagnet, the cyclotron was capable of producing 80 keV protons.

Beginning in 2008, two high school seniors, Peter Heuer and Heidi Baumgartner, began building a cyclotron [19] at Jefferson National Laboratory. Capable of producing protons up to 2.85 MeV at 2 mA of current, this cyclotron was to be used to produce positrons by colliding the protons into a stationary target.

Another use for small cyclotrons is radiocarbon spectroscopy. This was the motivation behind the University of California's "cyclotrino" [20]. Of particular interest in the dating of organic materials is the Carbon-14 isotope. Because ${}^{14}\text{C}$ has a different charge to mass ratio than other isotopes of carbon and nitrogen, the frequency of cyclotron resonance will be unique to ${}^{14}\text{C}$. Thus the cyclotrino is able to

accelerate only the ^{14}C for detection, allowing the fraction of ^{14}C in a sample to be measured and used to date objects from which the sample originated.

In addition to their value as vital physics machines, small cyclotrons can be used as an educational tool. Tim Koeth, an undergraduate physics student at Rutgers, wanted to build a cyclotron after learning about it in a sophomore physics course. With another classmate, Stu Hanebuth, construction began on the 12-inch cyclotron in 1995 [21]. The cyclotron, capable of producing 1 MeV protons, is used as part of an undergraduate Modern Physics Laboratory class at Rutgers as well as serving as a research tool [22].

The small cyclotron continues to be useful in the field. Whether it is used for low-energy nuclear physics, spectroscopy, of educational purposes, the cyclotron is still a useful tool in the modern age.

1.2.4 The Houghton College Cyclotron

Construction of the Houghton College cyclotron began in 2001, with the motivation of using deuteron-deuteron fusion in order to produce high energy neutrons [23]. These neutrons could be used in future neutron experiments. Such reactions could be achieved by accelerating deuterium gas in the cyclotron and letting the deuterons strike a deuterated polymer target. These deuterons would undergo either the $^2\text{H}(d,p)^3\text{H}$ or $^2\text{H}(d,n)^3\text{He}$ reaction, the former being unobservable since the protons will lose energy and stop in the chamber walls unless they are allowed to exit through a chamber port. The neutrons, however, could escape from the chamber and can be used in further scattering experiments.

High-yield resonances of other nuclear reactions could also be observed in the near future. The $^{19}\text{F}(p,\gamma)^{16}\text{O}$ and $^{31}\text{P}(p,\gamma)^{32}\text{S}$ reactions could be observed with the proton energy available to the cyclotron. The fluorine resonances occur at incident proton energies of 225, 230, and 340.4 keV with total cross sections of 0.173, 0.041, and 82-104 mb, respectively.



Figure 6. Photograph of the original cyclotron chamber taken in 2006. The copper dee and dummy dee can be seen, with the filament between being used to create ions. Figure taken from Ref. [25].

Originally, the Houghton College cyclotron chamber was constructed out of soldered brass, with the dee and dummy dee constructed out of copper plates, as can be seen in Figure 6. The cyclotron has gone through many designs, and was originally to employ a 0.5 T permanent magnet [24] whose strength was to be changed by altering the pole face separation.

Under an earlier design [25], consisting of a copper dee and brass chamber, the cyclotron briefly produced accelerated ions. After a few successful runs in 2007 a discharge from the dee to the chamber lid rendered the apparatus inoperable. After this, a new chamber was constructed out of aluminum. By 2009, resonances with up to 0.5 T fields were observed for hydrogen and helium, yielding up to 2 nA of current. No resonances could be observed above 0.5 T, and it was thought that this was due to the increased path length at high fields. It was hoped that lower pressures would allow higher energy resonances in fields up to the maximum of 1.1 T. This thesis will examine the improvements and performance of the cyclotron since 2009.

Chapter 2

CYCLOTRON THEORY

This chapter offers a survey of the theory behind the cyclotrons operation. Beginning with the derivation of cyclotron resonance, the issues of RF tuning, relativistic effects, path length, and methods of beam focusing will be discussed.

2.1 The Resonance Principle

2.1.1 Fundamental Frequency

As discussed in the previous chapter, cyclotrons utilize a low-voltage oscillating potential and an orthogonal magnetic field to accelerate particles in orbits of increasing radii. In order for acceleration to take place, the frequency of electric field oscillation must perfectly coincide with the frequency of the orbit of the particle within the chamber, a condition known as resonance. The frequency required for resonance can be found in the following way.

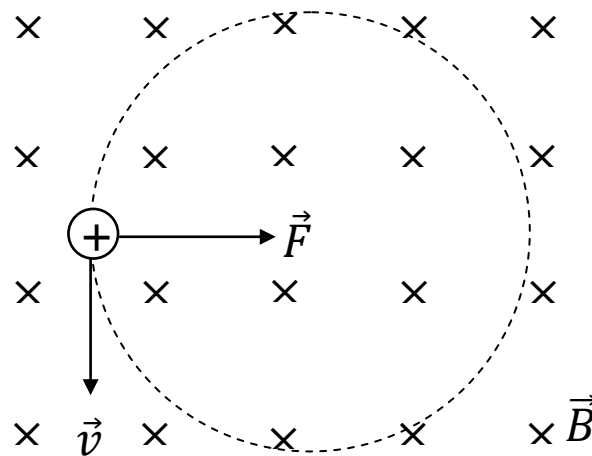


Figure 7. Force diagram for a charged particle moving in a magnetic field. A positively charged particle with velocity \vec{v} in a magnetic field of strength \vec{B} into the page, as shown, will experience a force that will constrain its motion to a circle.

As the particles drift within the electrodes $\vec{E} = \mathbf{0}$ because there are no electric fields inside a conductor. The force on a charged particle is given by:

$$\vec{F} = q\vec{v} \times \vec{B}, \quad (2.1)$$

where q is the particle's charge, \vec{v} is the velocity of the particle, and \vec{B} is the magnetic field. Since this is a cross product, the component of velocity orthogonal to the magnetic field will produce a force that is orthogonal to both \vec{v} and \vec{B} as shown in Figure 7. Thus the particles are constrained to helical orbits within the chamber. If the component of velocity in the direction of \vec{B} is assumed to be zero, then the particle orbit will be circular. In either case, the force required for an orbiting object of mass m to stay at a given radius r is given by

$$F = \frac{mv^2}{r}. \quad (2.2)$$

Since this centripetal force is provided by the magnetic field, we have the relation

$$qvB = \frac{mv^2}{r}. \quad (2.3)$$

Solving Eq. 2.3 for v and using the ion's circular orbit of total circumference $C = 2\pi r$, the period can be found

$$\tau = \frac{C}{v} = \frac{2\pi m}{qB}, \quad (2.4)$$

where, quite remarkably, that there is no radial dependence. This means that regardless of where an ion is in the chamber, it will have the same orbital period. Essentially, as the speed of the ion is increased in the acceleration gap, its half-orbit path length is also increased proportionally so that it will take the same amount of time to drift to the next acceleration gap regardless of its velocity.

In order to keep the particles in resonance, the dee voltage must be oscillated at a frequency equal to the orbital frequency:

$$f \equiv \frac{1}{\tau} = \frac{qB}{2\pi m}. \quad (2.5)$$

Here the linear relationship between magnetic field strength and frequency can be seen. If the cyclotron is operated at a fixed frequency f , the magnetic field strength associated with resonance at a given frequency is:

$$B = \frac{2\pi m}{q} f. \quad (2.6)$$

Thus ions with different charge-to-mass ratios will be in resonance at different magnetic field strengths for the same frequency. This accounts for the cyclotron's potential in the field of mass spectroscopy [7].

2.1.2 Harmonics

It might seem from Eq. 2.6 that there is only one magnetic field strength at which a particle can be accelerated with an acceleration frequency f , but consider a particle orbiting in such a way that the driving frequency can switch an odd number of times while it drifts freely inside the dee. Clearly, such a particle will continue to be accelerated at the driving frequency. An ion with orbital period $n\tau$ will remain in resonance, where n is any odd integer. This corresponds to an ion orbital frequency of f/n or for a fixed acceleration frequency, the field strength B/n , where B is the field strength associated with particles with orbital frequency f . The first two resonant frequencies, as well as the fundamental frequency, are shown in Figure 8.

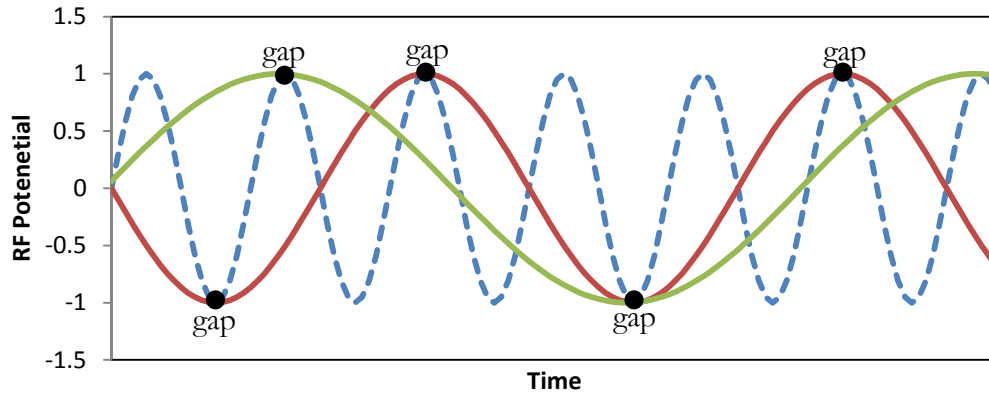


Figure 8. Harmonic frequencies of a cyclotron. The dotted line indicates the fundamental frequency in a magnetic field strength of B , which is the frequency at which the dees oscillate. A particle in a field $B/3$ will orbit at the frequency indicated in red. Since the potential is still properly oriented at the acceleration gap, the particle will stay in resonance. The same is true for the orbital frequency corresponding to $B/7$, shown in green, as well as any odd fraction of B .

2.2 Tuned LC Circuits

For a given B field, certain resonant frequencies exist that will cause the ions to be accelerated. To generate the required electric field, an alternating RF voltage is placed across the dees. This RF circuit can be generated using a tuned LC circuit.

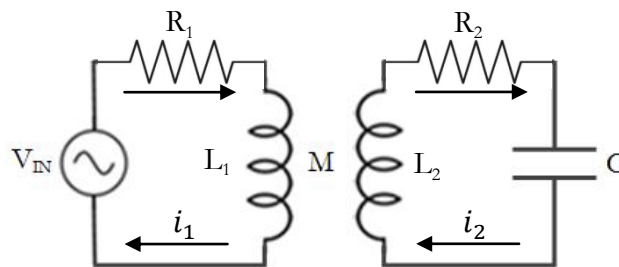


Figure 9. A coupled LC circuit. The AC voltage V_{IN} is coupled through mutual inductance M to the dee capacitance C . By adjusting the value for L_2 , the circuit can be made to resonate at a desired frequency.

For an LC circuit with a given inductance and capacitance, there is a frequency at which the system resonates. At this frequency power loss due to the impedance of the inductors and capacitors is minimized, allowing power to be delivered efficiently to the load. In the case of the cyclotron, the gap between the dee and grounded dummy dee and chamber walls provides the capacitance while an external inductor can be adjusted in order to tune the dee to oscillate efficiently at a selected frequency.

If an AC circuit with frequency ω and voltage amplitude E like that shown in Figure 9 with a total primary coil inductance L_1 , a secondary coil inductance L_2 , mutual inductance M and a dee capacitance C is being driven by an oscillating potential V_{in} , Kirchhoff's voltage law yields for each loop will yield

$$i_1 R - L_1 \frac{di_1}{dt} - M \frac{di_2}{dt} = V_{in} = E e^{j\omega t}. \quad (2.7)$$

$$i_2 R_2 + L_2 \frac{di_2}{dt} + \frac{\int i_2 dt}{C} - M \frac{di_1}{dt} = 0. \quad (2.8)$$

Where $V_{in} = E e^{j\omega t}$ represents the oscillating potential of the source voltage. The solutions to the above differential equations will be of the form

$$i_1 = A e^{j\omega t} \text{ and } i_2 = B e^{j\omega t}. \quad (2.9)$$

Substituting these into Eq 2.7 and 2.8 to find A and B results in

$$(A(R_1 + j\omega L_1) + B j\omega M) = E. \quad (2.10)$$

$$B \left(R_2 + j \left(\omega L_2 - \frac{1}{\omega C} \right) \right) - j\omega M A = 0. \quad (2.11)$$

Note that $Z_1 = R_1 + j\omega L_1$ and $Z_2 = R_2 + j\left(\omega L_2 - \frac{1}{\omega C}\right)$ are the complex impedances of loop 1 and loop 2, respectively. Using this, Eq. 2.10 and 2.11 simplify to

$$AZ_1 + Bj\omega M = E. \quad (2.12)$$

$$BZ_2 - Aj\omega M = 0. \quad (2.13)$$

Solving for A and B in Eq. 2.12 and 2.13 yields:

$$B = \frac{Aj\omega M}{Z_2}. \quad (2.14)$$

$$A = \frac{E}{Z_1 + \frac{M^2\omega^2}{Z_2}}. \quad (2.15)$$

Using these values in Eq. 2.9, the currents in each loop are

$$i_1 = \frac{E e^{j\omega t}}{Z_1 + \frac{M^2\omega^2}{Z_2}}. \quad (2.16)$$

$$i_2 = \frac{j\omega M E e^{j\omega t}}{Z_1 Z_2 + M^2\omega^2}. \quad (2.17)$$

Notice that $j\omega M$ is the impedance caused by the mutual inductance, henceforth denoted Z_m . Since these equations hold for all times, let $V_{in}(0) \equiv E'$. Eq. 2.16 and 2.17 become

$$i_1 = \frac{E'}{Z_1 - \frac{Z_m^2}{Z_2}}. \quad (2.18)$$

$$i_2 = \frac{E' M}{\frac{Z_1 Z_2}{Z_m} - Z_m}. \quad (2.19)$$

From Ohm's law we find that the voltage across the dee capacitance, V_c is given by

$$V_c = \frac{i_2}{\omega C} = \frac{E' M}{\omega C \left(\frac{Z_1 Z_2}{Z_m} - Z_m \right)}. \quad (2.20)$$

Since each impedance is complex, there are both real and imaginary components of V_c . The imaginary component can be shown to be

$$V_{cj} = \frac{E' M}{C} \left(\omega L_1 L_2 - R_1 R_2 - \frac{L_1}{C} - \omega^2 M \right). \quad (2.21)$$

When the circuit is in resonance, dee voltage is at a maximum and the imaginary component of the voltage is zero, which is satisfied when

$$\omega_r L_1 L_2 - R_1 R_2 - \frac{L_1}{C} - \omega_r^2 M = 0, \quad (2.22)$$

where ω_r is the resonance frequency. Solving Eq. 2.22, the resonance frequency for the RF circuit is

$$\omega_r = \frac{-L_1 L_2 \pm \sqrt{(L_1 L_2)^2 - 4M \left(R_1 R_2 + \frac{L_1}{C} \right)}}{2M}. \quad (2.23)$$

If L_1 and $M \ll L_2$, as in the Houghton College cyclotron, the resonance frequency can be approximated as

$$\omega_r = \frac{L_1 L_2}{M}. \quad (2.24)$$

From this it can be seen that by changing the values of L_1 and L_2 , the resonance frequency for the RF system can be adjusted.

2.3 Relativistic Considerations

The resonance principle described above ignores relativistic effects that affect an ion's motion. In order to be entirely accurate at high energies this effect must be considered.

The simplest way to correct for relativity is by considering the “relativistic mass” M of the ions, which is given by

$$M = \gamma m, \quad (2.25)$$

where m is the mass of the ion in the rest frame, and γ is

$$\gamma = \frac{1}{\sqrt{1 - \frac{v^2}{c^2}}}, \quad (2.26)$$

where v is the velocity of the ion relative to the laboratory frame. Hence, since

$$\tau = \frac{2\pi\gamma m}{qB}, \quad (2.27)$$

it follows that

$$f_r = \sqrt{1 - \frac{v^2}{c^2}} \frac{qB}{2\pi m} = \sqrt{1 - \frac{v^2}{c^2}} f. \quad (2.28)$$

where f is the classical frequency and f_r is the relativistic frequency.

Since relativistically there is a velocity dependence on orbital frequency, and the velocity is directly proportional to the orbit radius, for relativistic ions the orbital frequency depends on the beam radius.

In other words, the dee frequency would have to decrease as the ions' orbital radii increased. Thus a fixed-frequency cyclotron would require an altered dee geometry or an increasing B field in order to maintain resonance.

However, if $v \ll c$ then the frequency is very nearly the classically derived frequency. For the Houghton College cyclotron, a proton accelerated to the 400 keV will have a resonance frequency $f_r \approx 0.99957f$. Hence, relativistic effects are negligible for energies attainable in the Houghton College cyclotron.

2.4 Determining Ion Energy

For a non-relativistic particle of charge q traversing the electric field between the dees n times as it orbits, the kinetic energy gained is given by

$$T = \frac{1}{2}mv^2 = nqV, \quad (2.29)$$

where T is the ion's kinetic energy, V is the potential difference between the dees, and n is the number of times the particle has crossed the potential. Using Eq. 2.3, the kinetic energy of the ion is given by

$$T = \frac{q^2 B^2 r^2}{2m}. \quad (2.30)$$

Notice that the energy increases with the *square* of magnetic field and radius. Thus small increases in either parameter can result in large increases in the final energy of the particles. This can be seen in Figure 10.

Using the operating parameters for the Houghton College cyclotron, a magnetic field of 1.1 T and a maximum radius of 7.6 cm, theoretical maximum energies can be computed. For protons and double ionized helium energies up to 335 keV are theoretically possible, whereas deuterons and singly ionized helium could reach 167 keV and 84 keV, respectively. The use of a larger magnet supply and more

cooling water could increase the maximum field strength to around 1.2 T, enabling up to 400 keV protons to be obtained

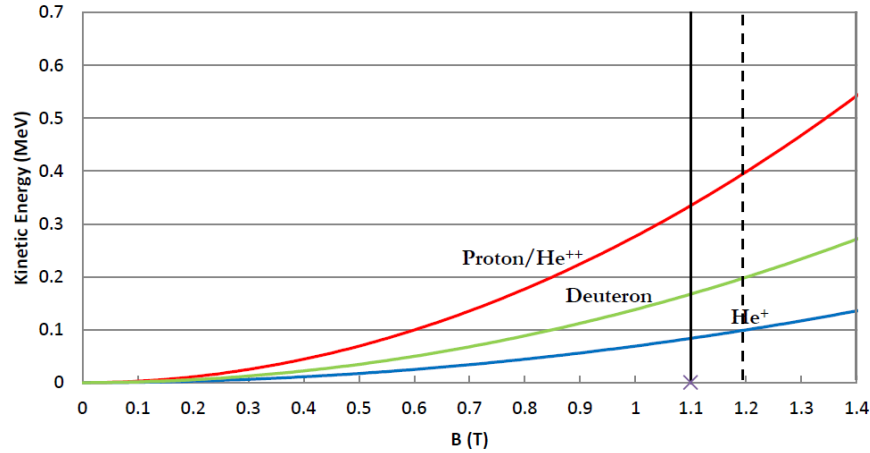


Figure 10. Graph of ion energies as a function of magnetic field using the maximum radius of 7.6 cm for the Houghton College cyclotron. The vertical line at 1.1 T represents the current limit for magnetic field achievable with the present electromagnet power supply. The 1.2 T dashed line represents the maximum field achievable with the 70 A power supply. Taken from Ref. [12].

2.5 Path Length

As the path length of a particle within the cyclotron increases, so too do the odds of interactions with gas within the chamber. Such interactions would cause the particle to fall out of resonance, so the mean path length is of particular interest. The radius of an orbit within the cyclotron is given by

$$r = \frac{mv}{qB}, \quad (2.31)$$

hence the radius changes with velocity. Using Eq. 2.29 it can be seen that

$$v = \sqrt{\frac{2nqV}{m}}, \quad (2.32)$$

where $n/2$ is the number of orbits. Using this, the radius of an ion orbit after l orbits is

$$r = \frac{m}{qB} \sqrt{\frac{2nqV}{m}} = \frac{1}{B} \sqrt{\frac{2nmV}{q}} = \frac{1}{B} \sqrt{\frac{lmV}{q}}. \quad (2.33)$$

If we assume the particles are constrained to circular (non-helical) orbits then the total distance, d , traveled by the particle is

$$d = \sum_{l=0}^N 2\pi r_l = \sum_{l=0}^N \frac{2\pi}{B} \sqrt{\frac{lmV}{q}}. \quad (2.34)$$

This equation is merely a useful approximation, since it assumes purely circular orbits as well as instantaneous accelerations. The latter approximation becomes increasingly accurate as the orbital speed increases, which occurs at larger radii, where more path length is accrued. So long as the dee separation is sufficiently small, this approximation is quite accurate.

2.6 Beam Focusing

As has been mentioned previously, in a homogenous magnetic field only those charged particles with no velocity component in the direction of the magnetic field would travel in circular orbits, otherwise the orbits are helical. Purely circular orbits are not possible to obtain in practice, since ions are produced with velocities in all directions. Without focusing, most of the ions will be lost when they collide with the dees or chamber wall. Fortunately, heterogeneity in the electric and magnetic fields within a cyclotron provide a means to focus the beam during the acceleration process.

2.6.1 Electrostatic Focusing

The electric field between the dees is responsible for the acceleration of the particles. An ion with charge q in an electric field \vec{E} will experience a force given by

$$\vec{F} = q \cdot \vec{E}, \quad (2.35)$$

with the force always in the direction of the electric field for positively charged ions. This is the force that accelerates the ions.

The electric field between the dees, however, is non-uniform. As can be seen in Figure 11, there will be some component of the electric field perpendicular to the plane of desired motion as well as in the direction of desired acceleration.

As the ion emerges from the dee, where it was shielded from electric fields, it encounters the field and is deflected as shown in Figure 11. The particle experiences a force toward the central x-z plane before it reaches the center of the gap as well, effectively focusing the ion toward the desired axis of motion. The ion will be defocused once it crosses the center of the acceleration gap. It would seem, since the magnitude of the vertical component of the velocity should be the same on either side of the center, that the focusing would be totally counteracted by the defocusing effect. However, the particle has been accelerating the whole time due to the horizontal component of the electric field, and will therefore spend less time in the defocusing region than the focusing domain- resulting in a net focusing effect.

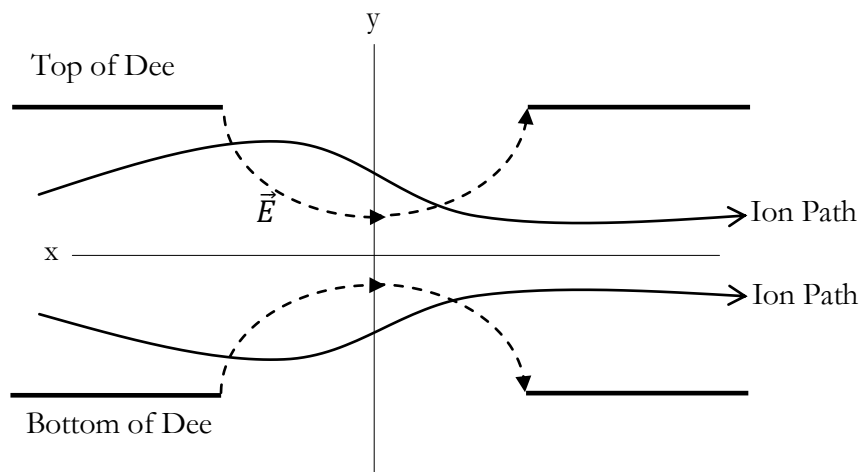


Figure 11. Diagram depicting electrostatic focusing. Ions enter the electric field and are focused by the y-component of the electric field while the x-component accelerates the ions. Once the ions pass the halfway point they will be defocused. Since the ions are accelerating, they will spend less time in the defocusing region, causing a net focusing effect.

Unfortunately, the overall effect of electrostatic focusing is small once the ion is moving fast at large radii. As the ions gain energy, their time spent in the accelerating region becomes smaller, reducing the effectiveness of electrostatic focusing as particle energy increases. Fortunately, for large radii magnetic focusing becomes important.

2.6.2 Magnetic Focusing

Much like the electric field, the magnetic field in the cyclotron is non-uniform. This heterogeneity enables the beam to be focused at higher energies. Recall that the force exerted on a charged particle in a magnetic field is given by

$$\vec{F} = q\vec{v} \times \vec{B}, \quad (2.36)$$

Because of the cross product, if the magnetic field is not perpendicular to the velocity, there will be both a radial and vertical component to the force as shown in Figure 12. The radial component of the magnetic field caused by fringe effects will, when crossed with the tangential velocity of the ion, cause the force on the ion to have a component toward the x-z plane, focusing the ion toward the central plane.

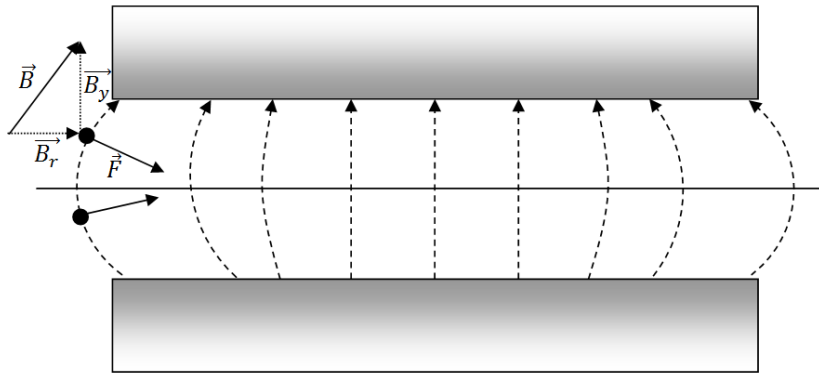


Figure 12. The focusing effect of a non-uniform magnetic field. A positively charged particle outside the central orbital plane will experience a force with a component toward the central plane caused by the radial component of the magnetic field crossed with the tangential velocity (in this instance, into the page) of the ion. This effect will be stronger at larger radii.

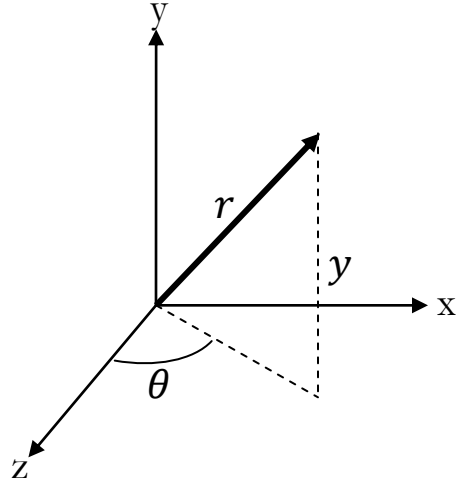


Figure 13. The cylindrical coordinate system used in this derivation. Here r is the distance of the ion from the center of the dees, θ is the angle in the x - z plane and y is the height above the x - z plane.

When the particle reaches the central plane, it will continue to drift past the plane and the process will be repeated on the other side. A vertical oscillatory motion can be predicted from the equation of motion. A thorough derivation of this motion can be found in Ref. [3]. Using the cylindrical coordinate system shown in Figure 13, the equation of motion in the y direction is given by

$$F_y = m\ddot{y} = Eq + q\dot{r}B_\theta + qr\dot{\theta}B_r, \quad (2.37)$$

The magnetic field strength on the fringe typically will decrease radially according to

$$B_y = B_0 \left(\frac{r_0}{r} \right)^n, \quad (2.38)$$

where B_y is the vertical magnetic field strength at radius r from the center, B_0 is the magnetic field strength in the central plane at the distance r_0 from the center, and n is a constant that depends on the particular magnet. Using Eq. 2.38, n can be found.

$$-(\ln B_y - \ln B_0) = n(\ln r - \ln r_0). \quad (2.39)$$

Taking the derivative of both sides yields

$$-\frac{dB}{B_y} = \frac{nr}{r}, \quad (2.40)$$

from which n is found to be

$$n = -\frac{r}{B_y} \frac{dB}{dr}. \quad (2.41)$$

Let $r = r_0 + \Delta r$ where Δr is small, such that $\frac{\Delta r}{r_0} \ll 1$, so that from Eq. 2.38

$$B_y = B_0 \left(\frac{r}{r_0}\right)^{-n} = B_0 \left(1 + \frac{\Delta r}{r_0}\right)^{-n}. \quad (2.42)$$

For such small oscillations, B_y can be approximated using a binomial expansion

$$B_y \approx B_0 \left(1 - \frac{n\Delta r}{r_0}\right). \quad (2.43)$$

Since the current density for the particle beam is very small, Ampere's Law is approximately

$$\vec{\nabla} \times \vec{B} = 0. \quad (2.44)$$

Solving for the θ component of the curl yields

$$\frac{\partial B_y}{\partial r} = \frac{\partial B_r}{\partial y}. \quad (2.45)$$

From this and Eq. 2.43 the radial component of the magnetic field is found to be

$$B_r = -\frac{nB_0z}{r_0}. \quad (2.46)$$

Substituting this into the Eq. 2.37, and neglecting the electric field, yields an equation of motion for y

$$m\ddot{y} = \frac{qvB_0ny}{r_0}. \quad (2.47)$$

Since $\frac{mv^2}{r} = qvB_0$ for resonance to occur, the following is obtained

$$\ddot{y} = \left(\frac{v}{r_0}\right)^2 ny \equiv \omega^2 ny, \quad (2.48)$$

which is the equation of motion for a harmonic oscillator, where the frequency of oscillation is

$$\omega_0 = \omega\sqrt{n}. \quad (2.49)$$

Hence the vertical motion of an ion in a magnetic field decreasing radially as Eq. 2.38 will resemble the motion of a simple harmonic oscillator with a frequency of

$$f_y = \frac{\omega}{2\pi}\sqrt{n} = f_0\sqrt{n}, \quad (2.50)$$

where f_0 is the resonance frequency of the cyclotron and f_y is the frequency of oscillations about the central plane.

The effect of magnetic focusing can be created whenever the magnetic field radially decreases. Thus it is often favorable to place ferromagnetic material between the magnet poles and the vacuum chamber in order to decrease field with radius and increase these desired focusing effects.

EXPERIMENTAL APPARATUS

3.1 Overview

This chapter presents an overview of the key systems in the Houghton College Cyclotron, shown in Figure 14.

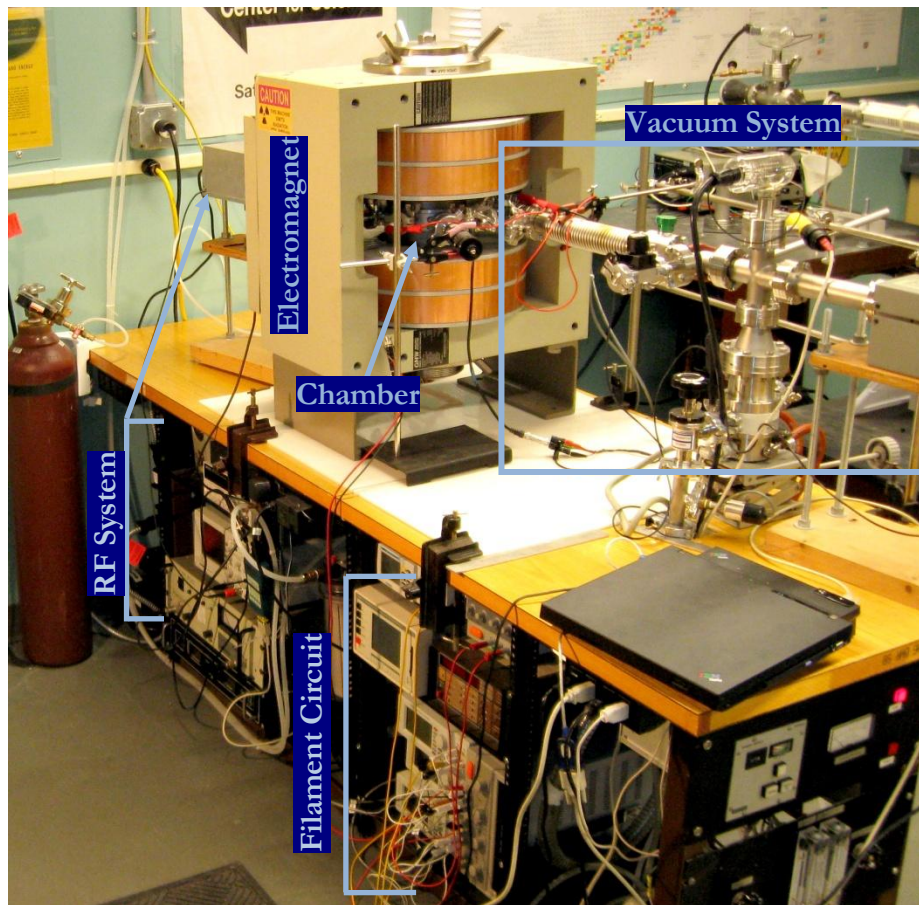


Figure 14. Photograph of the Houghton College cyclotron. The key systems: the RF system, electromagnet, vacuum system, filament circuit, and vacuum chamber are labeled.

The electromagnet, vacuum chamber, vacuum and gas handling system, filament, RF system, beam collector, and control system in their current configurations will all be discussed and potential improvements to some systems will also be explored.

3.2 Electromagnet

The cyclotron electromagnet is a GMW Associates 3473-70 with 15 cm diameter pole faces. With its adjustable pole gap, it allows for easy removal of the chamber. With the chamber between the pole faces the pole gap is roughly 3.85 cm and the highest magnetic field strength achievable using the PowerTen R62B-4050 magnet power supply is 1.13 T, as seen in Figure 15. Since this field corresponds to a 50 A current through the coils, the electromagnet must be water cooled at a rate of no less than 0.8 gal/min.

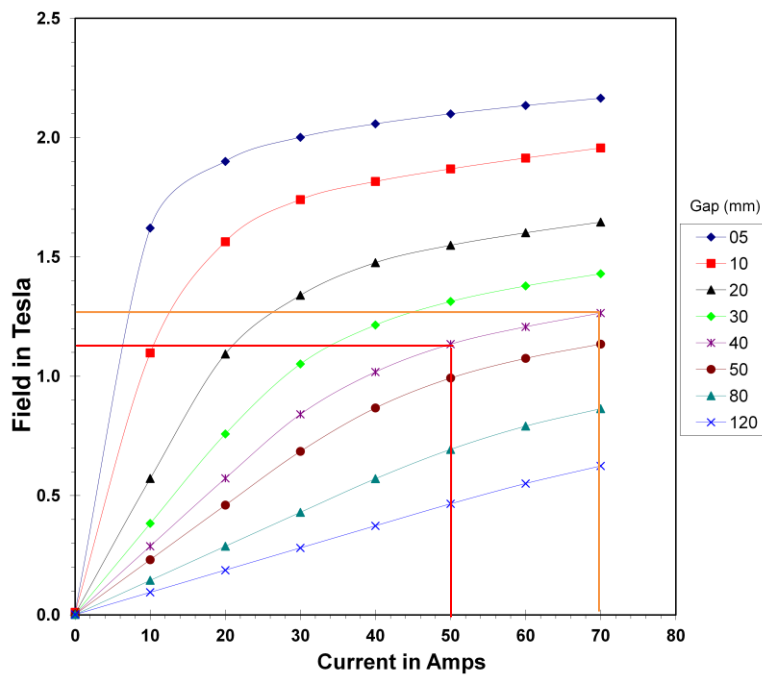


Figure 15. Plot of magnetic field strength as a function of current for varying pole gap separations using the GMW Associates 3473-70 electromagnet with the 15 cm pole faces. Using the present 50 A supply at a 4 cm pole gap will yield a maximum field of 1.13 T (red lines). Should a 70 A supply be used a 1.26 T field could be obtained during operation (orange lines).

Should a 70 A magnet power supply be purchased, the field strength could be increased to 1.26 T. Although this might seem like a small increase, recall that particle energy scales with the square of magnetic field strength. Hence, this field increase results in a 24% increase in maximum energy achievable.

The magnetic field for the electromagnet is monitored with a SMS Telatomic 102 gauss meter and a hall probe which fits between the pole face and chamber in a machined groove in the chamber lid. In order to test the accuracy of this meter, as well as obtain a field calibration, the magnetic field at various currents was measured using both the SMS 102 and a calibrated FW Bell 5070 Telsameter.

3.3 Chamber

The cyclotron chamber shown in Figures 14 and 16 was machined from 2.54 cm thick aluminum plate and has 10 evenly spaced 1.27 cm diameter ports attached with Hysol Loctite 1C vacuum epoxy to the chamber walls. The RF system, dummy dee ground, vacuum system, gas system, current collector, filament wires, and windows are connected to these ports. With a total outside diameter of 17 cm, the chamber slightly exceeds the electromagnet pole face diameter so that the edge of the dees is at the edge of the magnet poles.

The dee and dummy dee were constructed out of two 0.123 cm thick aluminum plates fastened to a 1.27 cm thick aluminum ring. The dees are held apart by ceramic spacers, with an acceleration gap of 0.635 cm. The dummy dee was cut to a width of 3.18 cm. The lids of the chamber consist of 0.65 cm thick aluminum plating with held by ten 2-56 ½ inch screws and sealed using 262 Viton o-rings that fit into machined grooves in the lid.

Figure 16 shows the chamber with the top lid removed. The dee and dummy dee can be seen. In between these two is the filament, whose glass base is visible. The filament is connected via barrels on top of a ceramic insulating sheet to wires that exit the chamber. The current collector is also visible.

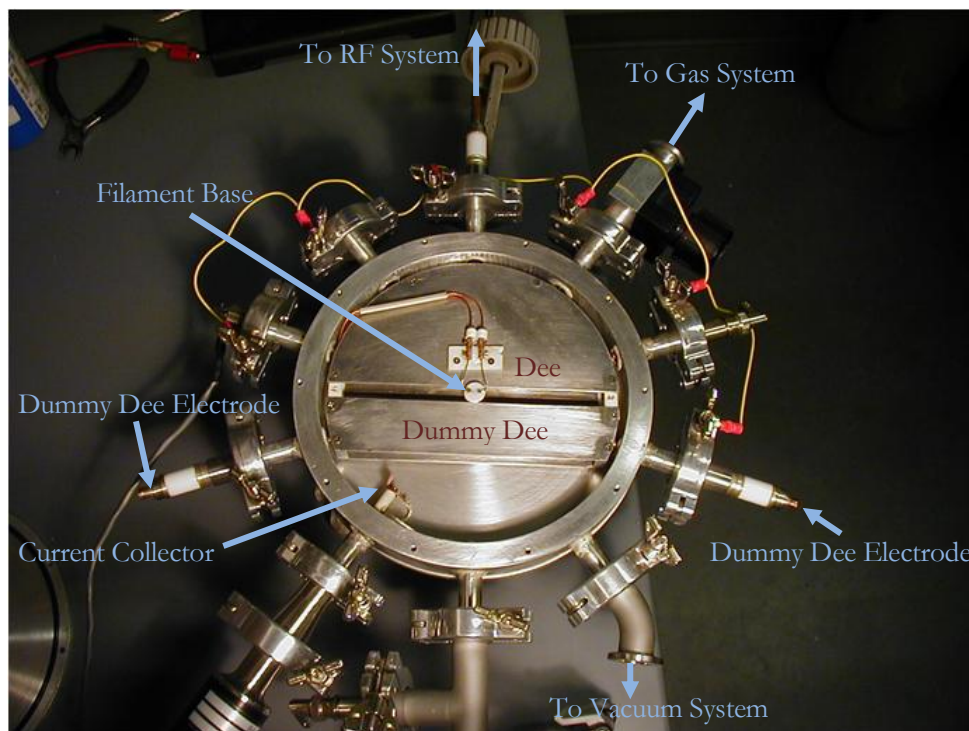


Figure 16. Photograph of the inside of the chamber. The dee, dummy dee, and filament base can be seen. Attached to ports are the current collector, electrodes for the dees, the gas system, and the vacuum system.

3.4 Vacuum and Gas System

In order to ensure sufficiently low pressures for successful operation, the Houghton College cyclotron utilizes a vacuum system, shown in Figures 14 and 17. First, a CIT-Alcatel 2012A rotary forepump is used to reduce the pressure to about 2×10^{-3} Torr and is measured with the CVT-272 convection gauge. The foreline pressure is monitored using a KJL-6000 thermocouple gauge. From there, a Pfeiffer TPU-062 turbopump is used to bring the pressure down to around the 2×10^{-6} Torr range with the pressures monitored by the Dunaway GP 275 ion gauge. In order to keep the turbopump from overheating, it is cooled with 18 °C water chilled with the Haskris Company A5H chiller at a flow rate of 0.2 gal/min.

Once the cyclotron has achieved this low pressure, hydrogen, helium, or a mixture is introduced until the system is at 10^{-6} to 10^{-5} Torr. Initially, a MKS 1179A Mass Flo Controller was used in order to precisely control the amount of gas present in the system. Unfortunately, one of the control pins became internally shorted to ground. At present, the Mass Flo Controller has been replaced with an Edwards LV10K leak valve. This system is less precise than the MFC and results in a fluctuation of gas pressure within the chamber over the course of a data run, which is undesirable for data collection where only one parameter should be varied at a time. The vacuum system also has numerous shutoff valves that allow different parts of the system to be isolated.

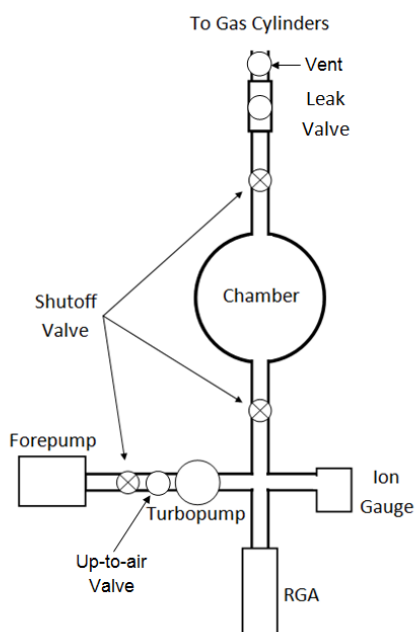


Figure 17. Schematic of the vacuum and gas system for the Houghton College cyclotron. Pressures as low as 10^{-7} Torr may be achieved using the rotary forepump and turbopump before gas is introduced to 10^{-6} Torr for ionization and acceleration in the chamber. Pressure is monitored via an ion gauge and gas content is measured using the SRS RGA 100.

In order to measure the partial pressure of the gasses within the cyclotron, a SRS RGA 100 Residual Gas Analyzer (RGA) is used. The RGA is a mass spectrometer, which measures the partial pressure as

a function of atomic weight. This allows the relative amount of hydrogen and helium to be measured as well as water vapor and air which is an indicator of a small leak.

At present, the RGA is not calibrated and cannot be used to measure the absolute pressures for element. Thus only the relative pressure for each gas can be obtained while the Ion Gauge is used to monitor the total pressure.

3.5 Filament

In order to ionize the gas inside the chamber for acceleration, a tungsten filament similar to the Kimball physics ES-020 is placed between the dees. The filament ionizes gas via thermionic emission. The hot filament ejects electrons due to thermal energy. If the filament is held at a sufficiently large negative voltage, these electrons will be accelerated away from the filament. The electrons will lose energy by ionizing atoms in the gas. Since these ions have charge, they can be accelerated in the cyclotron.

In the Houghton College cyclotron, the filament is typically held at -90 V, though the bias appears to have little influence on the beam current. This bias is created using two Unisource PG100 programmable power supplies. The potential across the filament is ~2 V at a current of up to 2 A and is created using a RSR HY3003 power supply. Since the tungsten filament used is very thin (0.13 mm in diameter) the voltage had to be limited so that the voltage would not increase as the tungsten got thinner, which would lead to a more rapid burn out of the filament. If the current is much higher, the filament will blow out or suffer a reduced lifespan.

The filament, which is mounted on a glass base, is placed in the center of the chamber between the dee and dummy dee and is shown in Figures 14 and 16.

3.6 RF System

One of the systems critical to the function of a cyclotron is its tuned RF circuit, which efficiently supplies the acceleration voltage at a desired frequency. The circuit can be tuned in order to operate

over a vast range of frequencies, corresponding to resonances at different magnetic field strengths and therefore different energies.

The Houghton College cyclotron's RF system is shown in Figure 18 and consists of a function generator, RF power amplifier, antenna auto tuner, mutual inductors, and the dees themselves.

The HP 33120A function generator provides the sinusoidal RF voltage at frequencies up to 15 MHz at a range of peak-to-peak voltages, usually set from 100mV to 350 mV. This signal was then amplified by a ENI 155LCRH RF power amplifier to increase the power to as much as 100 W, although the cyclotron typically operates using 30 W of RF power and can be monitored using the Bird 43 A RF power meter.

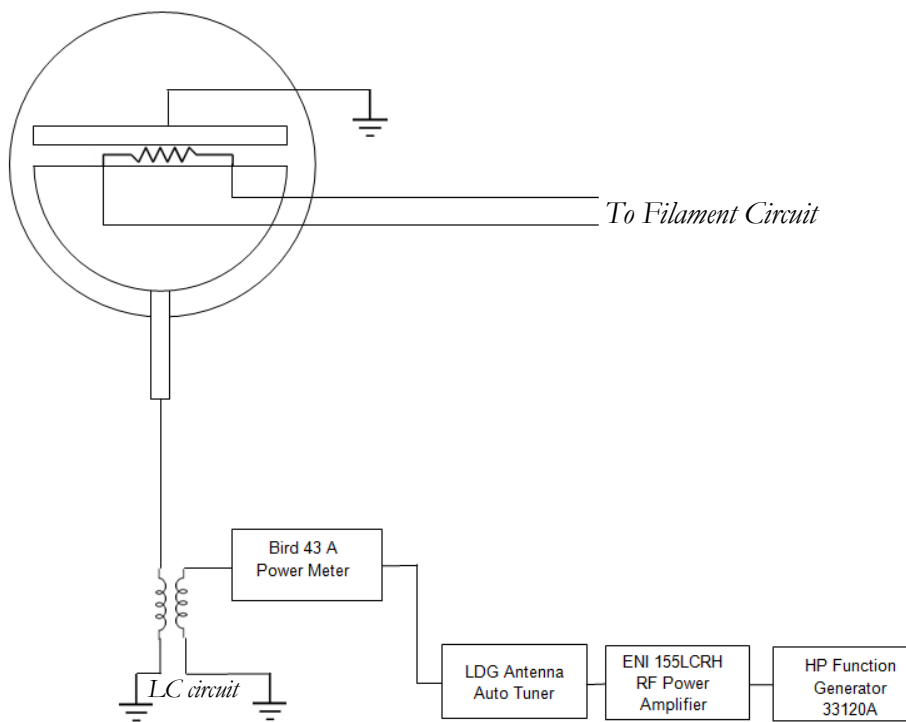


Figure 18. The Houghton College cyclotron RF system. A function generator produces a sinusoidal waveform at the desired operating frequency which is then amplified. The inductors in the tuned circuit from Section 2.2 can be adjusted to bring the circuit near resonance while the antenna auto tuner adds small amounts of capacitance to the circuit to fine-tune the resonance of the circuit.

At this point, ideally, the voltage would drive the primary side of the LC circuit described in Section 2.2. However, it is difficult to adjust the inductance to perfectly match the output impedance of the RF amplifier. In order to achieve the best tune the system includes the LDG AT-200PC auto tuner. This instrument adds small amounts of capacitance and inductance in order to ensure the most power is delivered to the dee and is not reflected back into the RF amplifier. Thus, the inductance of the circuit is adjusted to obtain a coarse tune and then the frequency tuner is used to match the RF amp output impedance and thereby reduce reflected power.

Figure 19 shows an earlier version of the coils which used a variable inductor for the secondary coil. The RF input could be attached to the primary coil in any one of several locations so as to vary the number of turns. The secondary coil was a variable inductor whose number of turns could be more finely controlled.

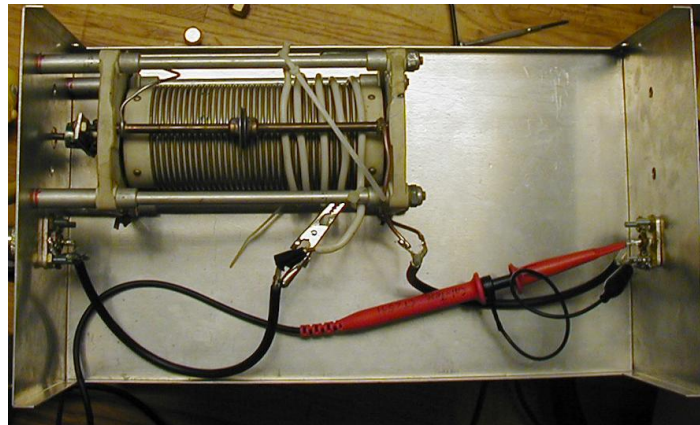


Figure 19. The previous LC circuit inside a grounded shield box. The RF input passed through the primary coil (insulated white coils) and was passed via mutual inductance to the variable inductor of the secondary coil, which is connected to the dees within the chamber. Also pictured is the HV oscilloscope probe for measuring the dee voltage.

For lower frequencies of operation this system worked well. The reasons why this system had to be replaced were twofold. In order to obtain higher frequencies, the inductance of the circuit must decrease. Because the coils on the secondary were so close together, frequencies up to 15 MHz

would require so few that it was impossible to get the primary coil around them. Secondly, as the voltage was increased the primary coil sparked to the secondary.

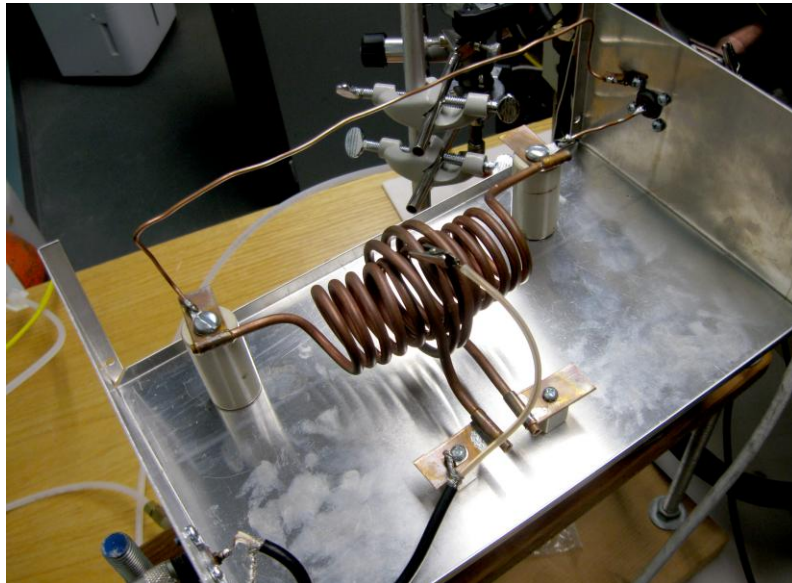


Figure 20. The new LC circuit inside a grounded shield box. The coils are made from bent 1/4 inch refrigerator copper tubing. The RF input passes through the primary coil (outer copper windings) and was passed via mutual inductance to the variable inner secondary coil, which is connected to the dees within the chamber.

Figure 20 shows the new system which uses coils made from bent refrigerator copper tubing. Both the primary and secondary coils can be removed and replaced with ones with different numbers of turns in order to adjust the resonance frequency and input impedance of the circuit. This system does not have the sparking problem of the previous system. Further, higher frequencies can be easily obtained by proper choice of coils. This is the system that was used during the highest frequency runs yet achieved on the cyclotron.

The RF system, as well as the rest of the cyclotrons systems, are grounded only through an electrical outlet ground. This lack of a dedicated ground may have caused a ground loop resulting in a $10 V_{pp}$

voltage on the filament circuit. To overcome this issue a dedicated good earth ground has been installed in the laboratory for scientific equipment such as the cyclotron.

3.6.1 RF Tuning

In order for the cyclotron to operate the RF circuit must be tuned to resonance for the selected frequency. The following is a description of how the tuning is achieved on the cyclotron.

First, a dee frequency is selected based on the desired ion energy. Next the dee capacitance is measured using a BK 8786 LCR meter. From this, an inductance is determined for the secondary coil that corresponds to the desired resonance frequency and the corresponding coils are installed in the shielded box. Using the LCR meter the inductance is measured and the input to the secondary is adjusted until the inductance is near the desired value and the primary is adjusted to minimize the reflected RF power. To ensure the circuit is resonant near the desired frequency, the system is attached to the AEA VIA Bravo II which measured the SWR and impedance as a function of frequency. Selecting a suitable range of frequencies around the desired frequency on the device, a scan of frequencies is performed.

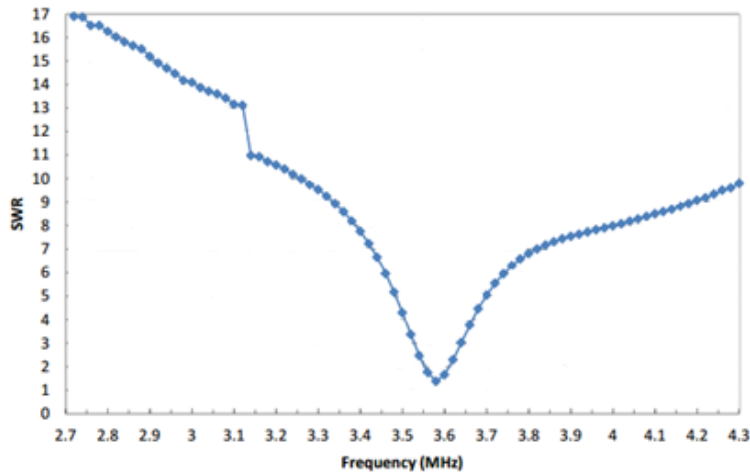


Figure 21. Graph of SWR versus frequency obtained from the AEA VIA Bravo II. This graph indicated that the best tune is in the $f = 3.57$ MHz area.

The standing wave ratio (SWR) and total impedance are examined on the resulting plot as shown in Figure 21. The SWR indicates the ratio between amplitudes of the highest and lowest voltages in the RF circuit. The ideal value, corresponding to perfect transmission and no reflected power, is 1:1 and occurs when the input impedance matched the output impedance. Once the final adjustments to the coils have been made, the lid is attached to the shielded box. The LDG antenna auto tuner is used to add small values of capacitance and inductance to the primary RF circuit in order to reduce the SWR to the lowest value possible.

Beginning with a low function generator amplitude output (i.e. 50 mV), the signal dee voltage is measured via the oscilloscope probe pictured in Figure 19. The function generator frequency is then raised in small increments and the dee voltage is noted at each setting, resulting in a plot like the one in Figure 22. The frequency corresponding to the highest dee voltage output is selected for the next stage of the tune.

As a final step, the function generator voltage is incremented and the dee voltage according to the probe is recorded in order to obtain a voltage calibration, as shown in Figure 23. This is done until the dee voltage is around 3000 V, as any further might result in sparking between the dee and dummy dee.

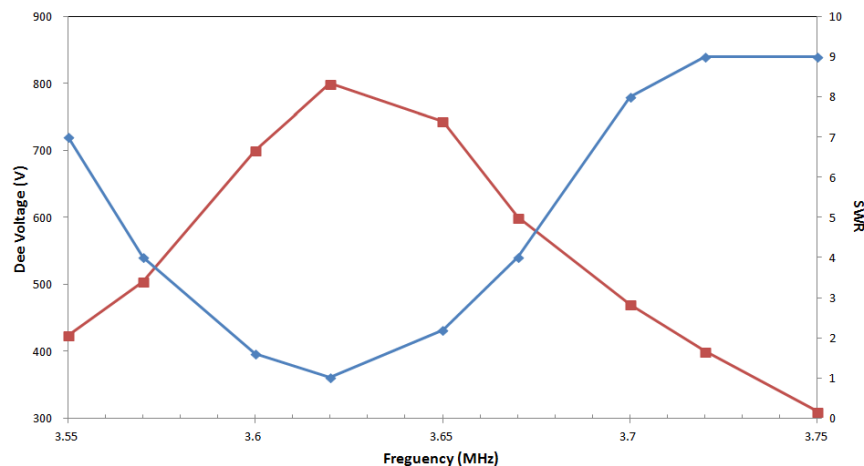


Figure 22. Graph of SWR (blue) and dee voltage (red) as a function of frequency obtained by hand by varying the FG frequency and making note of the measured SWR according to the LDG AT-200 PC auto tuner. Here the best tune corresponds to $f=3.62$ MHz

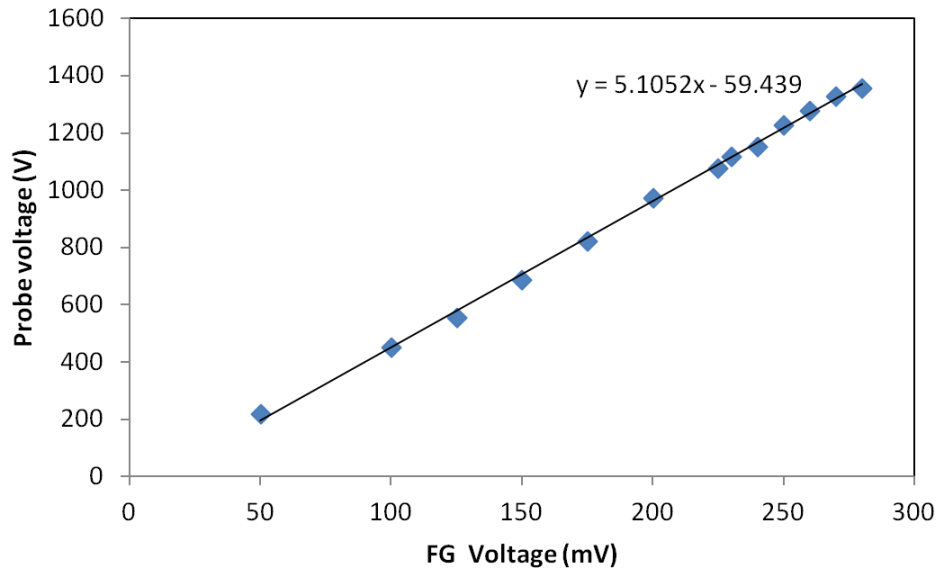


Figure 23. Voltage calibration for a $f=5.8$ MHz tune. The function generator voltage was incremented and the oscilloscope probe voltage was noted at each step. Note the linear relationship, given by the equation shown.

3.7 Beam Collector

The current collector is a small, angled copper sheet attached to a threaded ceramic tube. As ions are accelerated in the chamber their radii of orbit increases and they will collide with the copper sheet, and create a small current that is passed through a shielded BNC coaxial cable to another port where it is read out by a Keithley 617 electrometer. The current collector is connected to a linear motion feedthrough that can be adjusted while the chamber is between the magnet pole faces, enabling the measurement of beam current at varying radii.

The recorded current is not solely the ion beam, however. An ion colliding with the collector may eject secondary electrons which escape and are therefore counted as positive current resulting in a higher current reading. To prevent this, a bias circuit was created to attract secondary electrons and is shown in Figure 21. A 9V bias on the current collector will reduce the number of electrons from being escaping, allowing the current measured to accurately reflect the ion beam current. Ideally, a Faraday

cup would be used to measure the beam current with higher precision and is a future modification that can be made to the cyclotron.

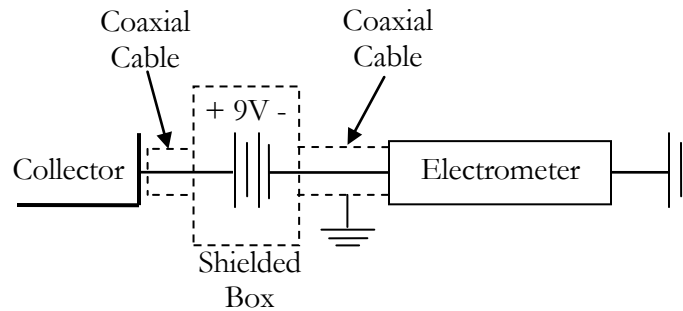


Figure 24. Beam collector circuit diagram. The 9V potential reduces the escape of secondary electrons, allowing for a more accurate measurement of beam current.

3.8 Control System

Most of the key systems of the Houghton College Cyclotron can be controlled or monitored remotely using National Instrument's LabVIEW 7.0 software and a GPIB-Enet-10 converter. The magnetic field strength can be varied as well as measured, while the beam current and pressure can also be read remotely. This allows the user to be in separated room from the cyclotron during data runs, which allows for more precise measurements of the small beam currents. In the future, isolation of the cyclotron may be required to perform nuclear physics experiments.

The LabVIEW program allows the user to perform magnet scans at a fixed dee potential and frequency. After inputting the maximum magnet supply current the program is run and the beam current according to the Keithley 617 Electrometer and magnetic field according to the SMS 102 Gauss meter are recorded as the magnet current is incremented up to the set maximum. The block diagram for the program can be found in the Appendix.

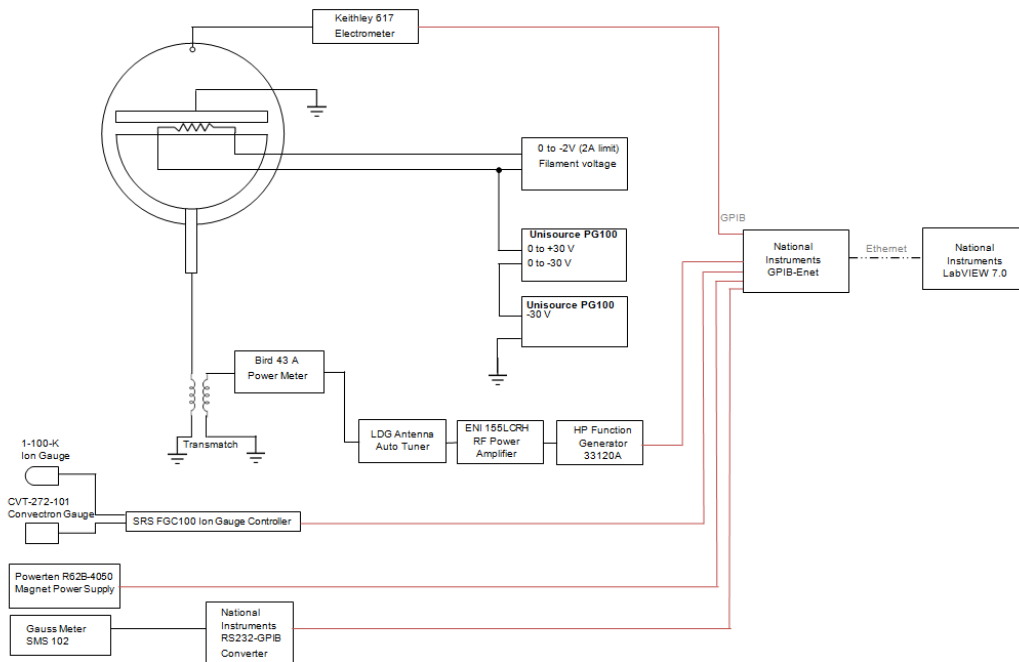


Figure 25. Block diagram of the control system. Using LabVIEW 7.0, the electromagnet field strength can be remotely controlled. In addition, the beam current, magnetic field strength, and pressure can be monitored remotely.

Chapter 4

RESULTS & DISCUSSION

The Houghton College cyclotron is currently working, and has been used to collect data for varying operational parameters. Beam current as a function of dee voltage, gas pressure, filament float voltage, and current collector radius has been measured. These measurements will aid in maximizing beam current for future experiments.

4.1 Magnet Scans

In order to examine the resonances, the magnetic field was incremented and the beam current was recorded. At certain magnetic field strengths resonance occurred and the beam current reached a maximum.

Figure 26 shows a cyclotron scan at 3.68 MHz with a filament bias of -91 V and the current collector at a radius of 55.6 mm. The dee voltage was 2000 V_{pp} and the pressure started at 2.5×10^{-5} Torr with equal parts hydrogen and helium. A labeled vertical line indicates the theoretical location of a resonance B or while unlabeled indicates a resonance at B/3, B/5, and so on. Included is a full scan out to 1 T. It can be seen that the location of current spikes at a given field strength always occur at or very near the theoretical resonances. The discrepancies could be the result of a lack of accuracy in the magnetic field sensor calibration.

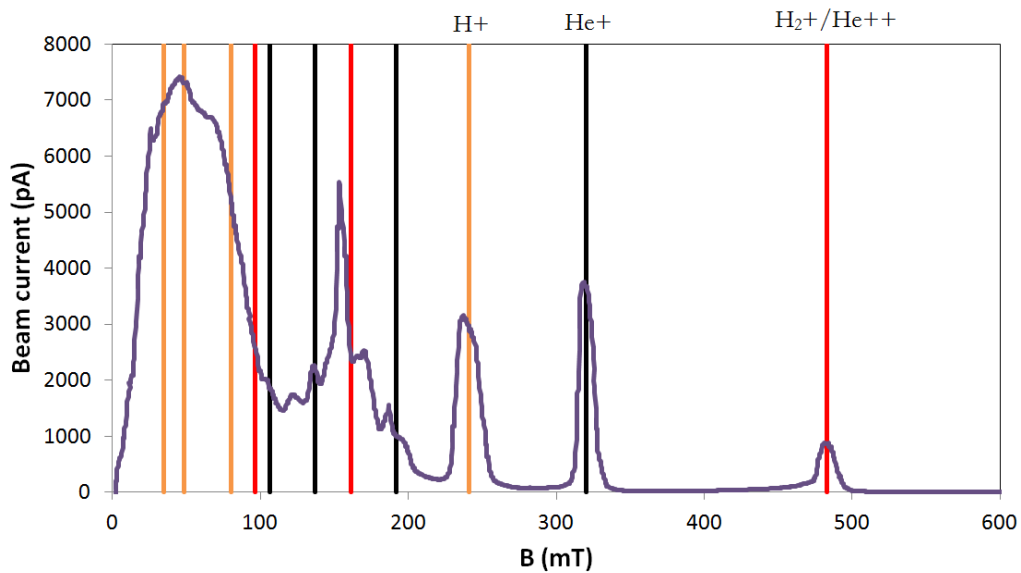


Figure 26. Plot of a magnet scan at $f=3.68$ MHz. The plot is beam current in pA as a function of magnetic field strength in mT. Vertical lines indicate the theoretical location of resonance peaks for hydrogen (orange), helium ions (black), and doubly ionized helium or ionized molecular hydrogen (red) at this cyclotron frequency. The labeled lines represent the primary resonance field strength while the others represent the resonance at $B/3$, $B/5$, etc.

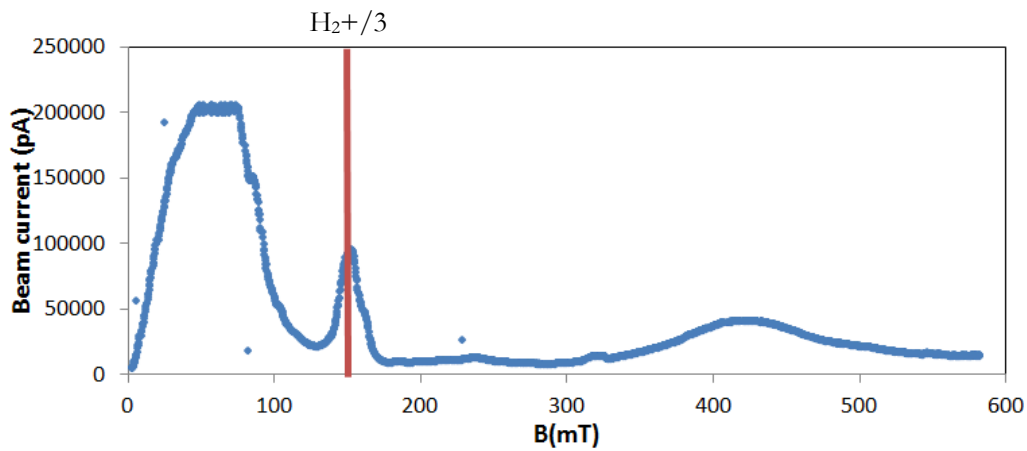


Figure 27. The highest beam current recorded to date within the Houghton College cyclotron. At a dee frequency of 3.62 MHz at 2000 V_{pp} with the filament floating at -90 V, a peak approaching 100 nA at the theoretical $H_2^+/3$ resonance (red line) is observed. Note that the resonance peaks are much broader due to the high pressure within the chamber.

During one early run the highest beam current achieved to date was measured. The gas pressure at the time of the run was about 10^{-4} Torr. The run with only hydrogen, at a frequency of 3.62 MHz and dee voltage of 2000 V_{pp} with the filament floating at -90 V, showed close to a 100 nA peak at 149 mT – corresponding to the 1/3 the field strength of the molecular hydrogen resonance ($H_2^+/3$), is shown in Figure 27.

4.2 Effect of Filament Bias Voltage

One parameter that can be adjusted on the cyclotron is the negative bias at which the filament is held. Since the lowering the bias should reduce the velocity of the electrons emitted from the filament, it was thought that this would reduce the number of ions within the chamber and therefore result in a reduction in beam current.

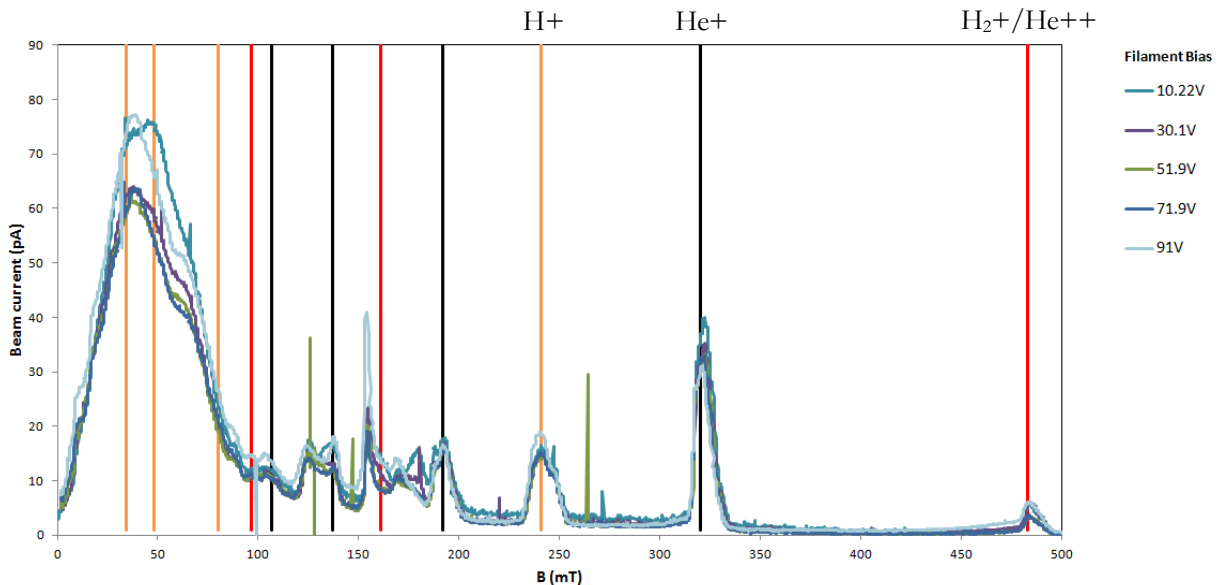


Figure 28. Effect of filament bias on beam current. At a constant operating frequency, pressure, current collector radius, and dee voltage a series of scans were performed at varying filament biases. As before, the vertical lines indicate theoretical resonance locations. It appears that filament bias has no effect on the beam current.

Magnet scans at a dee frequency of 3.67 MHz at 2000 V_{pp} were performed with the current collector at a constant radius of 63.8 mm for varying filament biases. Although the leak valve does not allow constant pressure beam current readings were taken within the pressure range of 1.2×10^{-5} to 1.5×10^{-5} Torr with equal quantities of hydrogen and helium. The results are displayed in Figure 28, which show that filament bias does not seem to have a significant effect on the beam current.

4.3 Effect of Dee Voltage

The dee voltage does not change the overall energy of particles but it will determine the overall path length of an ion in the acceleration chamber by determining the number of orbits required to reach a given beam radius. The greater the dee voltage, the fewer orbits an ion must undergo and the shorter the overall distance to reach a given radius of.

The longer a particles path, the more likely it is that it will interact with a gas atom in the chamber and possibly fall out of resonance. For this reason, the beam current should increase with increasing dee voltage. In order to test this, a series of scans with varying dee voltages were performed at 3.65 MHz and a current collector radius of 63.8 mm at pressures ranging from 2.3 - 2.5×10^{-5} Torr with only hydrogen. Along with the full scans, the beam current at two resonance peaks (the H₂⁺/3 160 mT and H⁺ 240 mT peak) was plotted as a function of dee voltage. The results are shown in Figure 29.

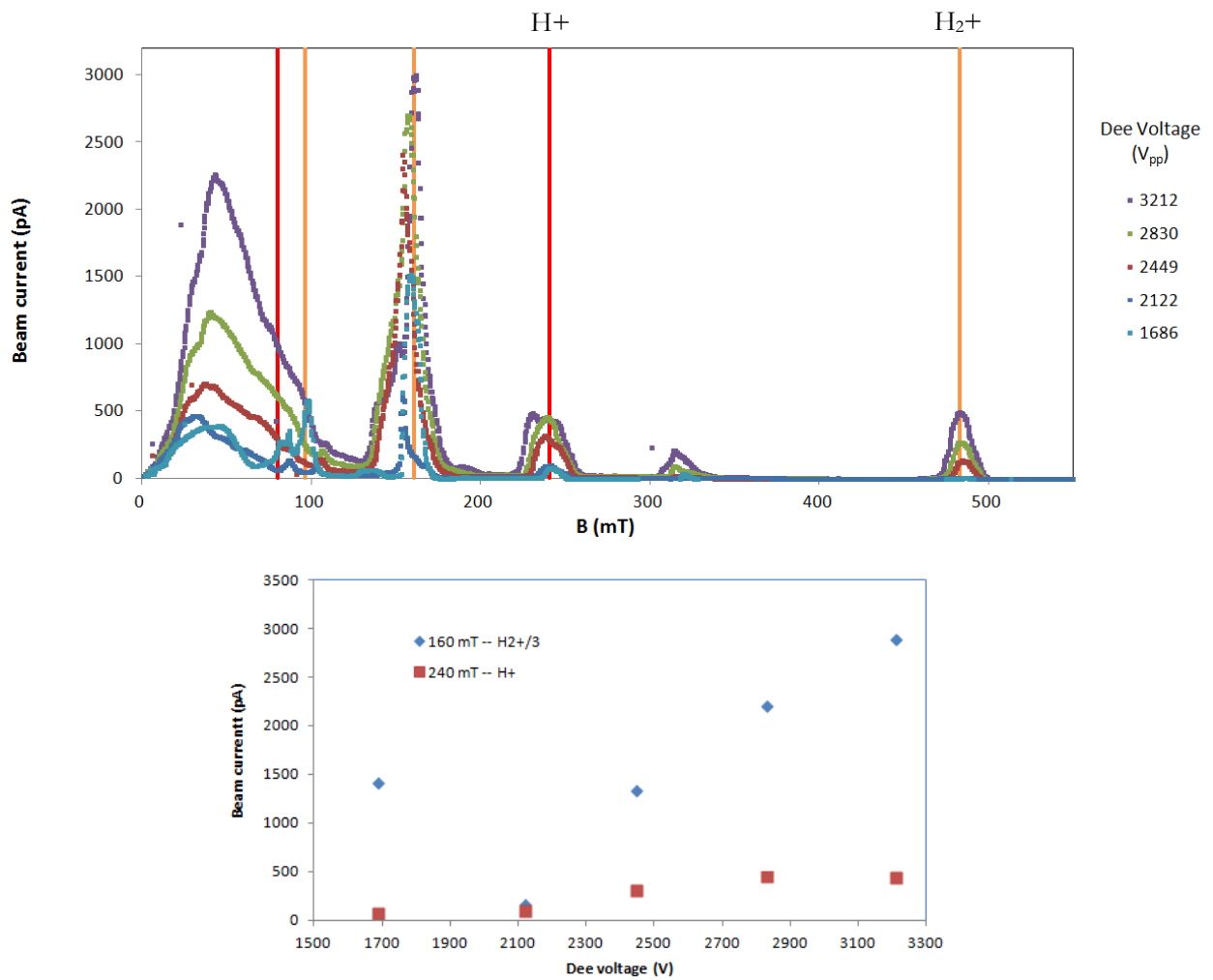


Figure 29. Effect dee voltage bias on beam current. At a constant operating frequency, pressure, and current collector radius a series of scans with hydrogen were performed at varying dee voltages. The top graph represents the full scans while the bottom plot is the effect of dee voltage on beam current at two resonance peak locations. It can be seen that in general, an increase in dee voltage results in a higher beam current.

4.4 Pressure Effects

The gas system of the cyclotron allows for a wide range of pressures within the chamber. There is a tradeoff involved in determining the best operating pressure. If there is too little gas, less ionization will occur resulting in a reduction of beam current. Too high a pressure and the ionized particles will likely interact with gas inside the dee and fall out of resonance. In order to determine the effect of gas pressure on beam current, a series of magnet scans, shown in Figure 30, were performed at a dee voltage of 2000 V_{pp} oscillating at 3.62 MHz for varying gas pressures. Initially, only hydrogen was used but helium was introduced into the system for the three lowest pressure runs. It is important to note that these pressures are read with the uncalibrated RGA and are therefore only relative pressures.

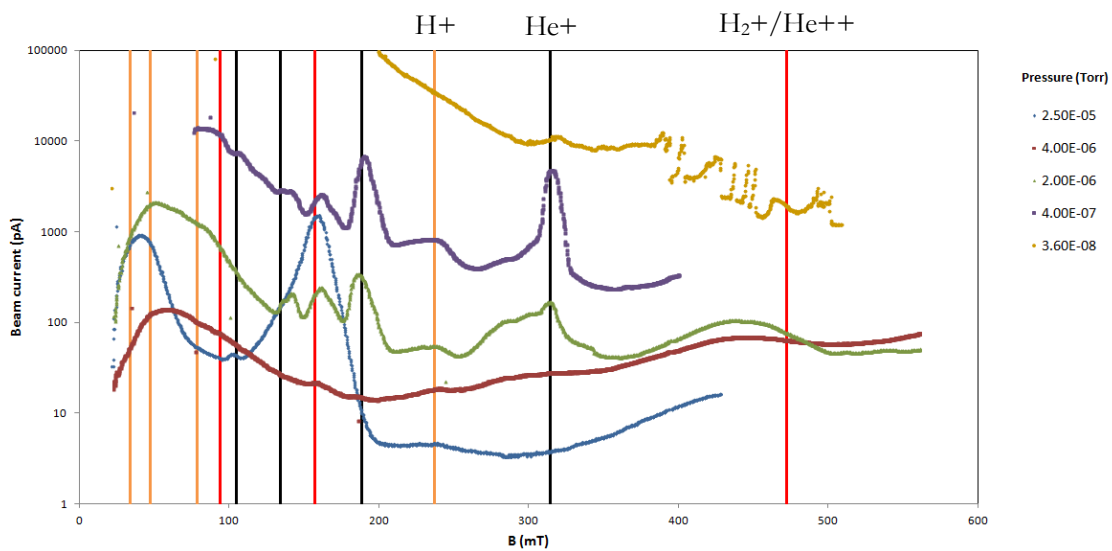


Figure 30. Effect of gas pressure on beam current. At a constant operating frequency, dee voltage, and current collector radius a series of scans with hydrogen were performed at pressures. After the two highest pressure runs with only hydrogen, helium was introduced into the system. As pressure is lowered it appears that beam current increases and peak resolution improves. The higher peak in the highest pressure run could be because so much ionization occurred that it overcame the negative effects of gas collisions. In addition, the well defined peaks at the lowest pressure might be caused by the very low rate of ionization.

At sufficiently high pressures, large amounts of ionization result in high current resonance peaks, though they are broadened greatly due to the interactions occurring with non-accelerated gas. As the pressure is lowered the beam current in the peaks first drops then rises again steadily with improved resolution. The initial drop is likely due to the reduce ionization rate while there is still high levels of gas interaction that causes a loss in resonance. Once there are sufficiently fewer gas atoms to interact with, the current will rise again- this time with improved resolution due to little or no interactions during acceleration. The lowest pressure scan shows poor resonance peaks, which is probably due to insufficient ionization.

4.5 Beam Current at Varying Collector Radii

Another characteristic that can be measured in the Houghton College cyclotron is how the beam current changes as a function of current collector radius. At a constant dee voltage of 2000 V_{pp} oscillating at 3.68 MHz at pressures ranging between 1-3.3x10⁻⁵ Torr with equal parts hydrogen and helium, the series of magnet scans shown in Figure 31 were performed. Starting at the largest radius, each successive scan was taken at a smaller current collector radius. In Figure 32, the magnet was also set to a field of 320 mT (He⁺/3 resonance) and the beam current was recorded at varying radii.

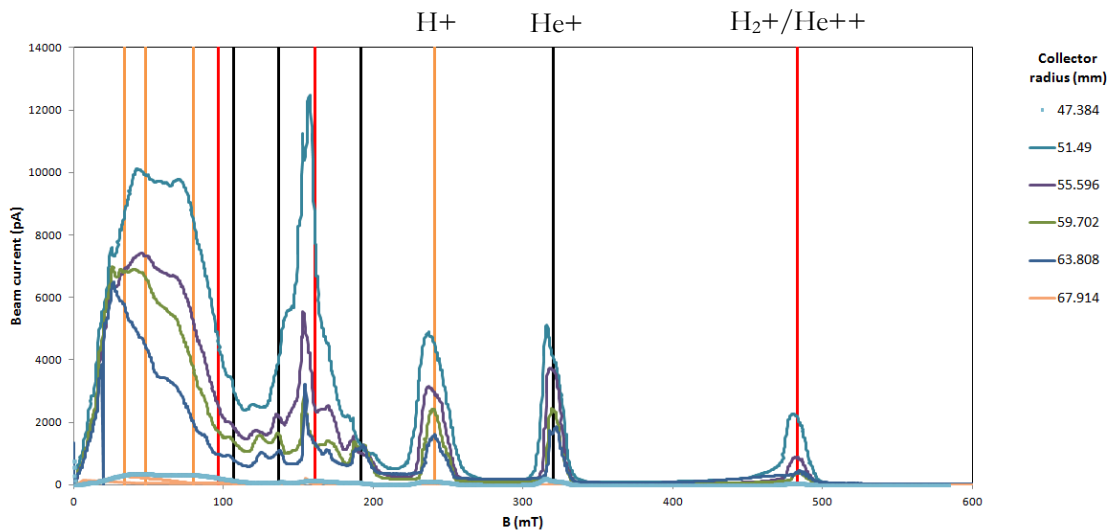


Figure 31. Full scans at different current collector radii. In general, the beam current increases with decreasing radii because of the shorter path length. The lack of current at 47.38 mm, which is just inside the dummy dee, is not understood at present.

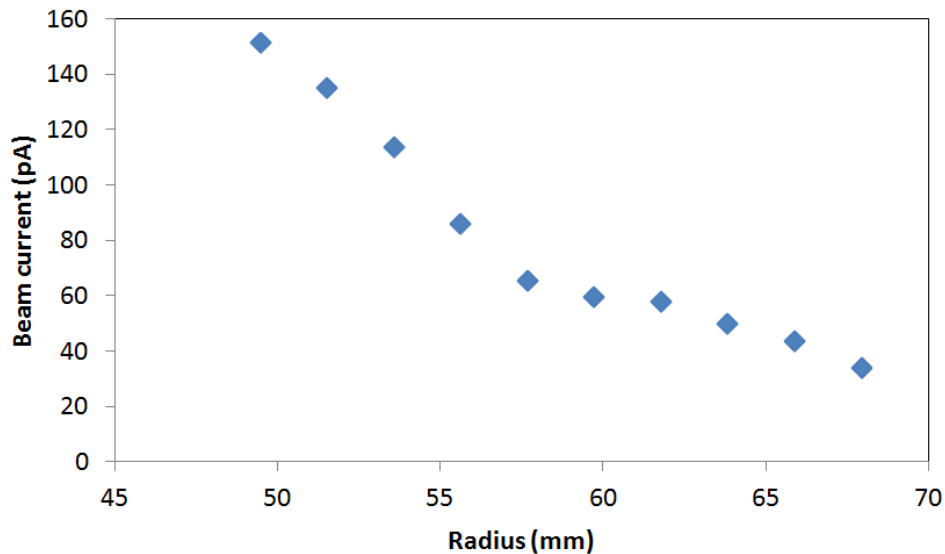


Figure 32. Beam current as a function of collector radius. Set to the $\text{He}^+/3$ resonance, the current on the collector was measured at a series of radii. Clearly, much of the beam current is being lost by the time the beam reaches larger radii.

As the radius of the current collector decreased, an increase in beam current was noted. The reasons are twofold. First, the path length for the ions is short so the chance of interactions with the gas molecules within the dees is smaller. Secondly, the particle beam has had less time to defocus before colliding with the current collector. The smallest radius, corresponding to the current collector being located inside the grounded dummy dee, had little to no beam current.

One way the loss of beam current could be reduced is by shaping the magnetic field to increase the effects of magnetic focusing. This could be done by adding shims of ferromagnetic material between the chamber and pole faces. Presently, a simulation of the cyclotron is being developed in order to determine how such shims would be placed to shape the beam for the future goal of increasing magnetic focusing effects.

4.6 Increasing Frequency

In order to obtain the maximum energy from the cyclotron, the LC circuit must be tuned so that cyclotron resonance occurs at the maximum magnetic field strength. For protons (H^+) to be in resonance at the maximum field of 1.13T a frequency of 17.23 MHz must be achieved, which will require a different function generator than the one currently in use, and will result in a maximum kinetic energy of 335 keV.

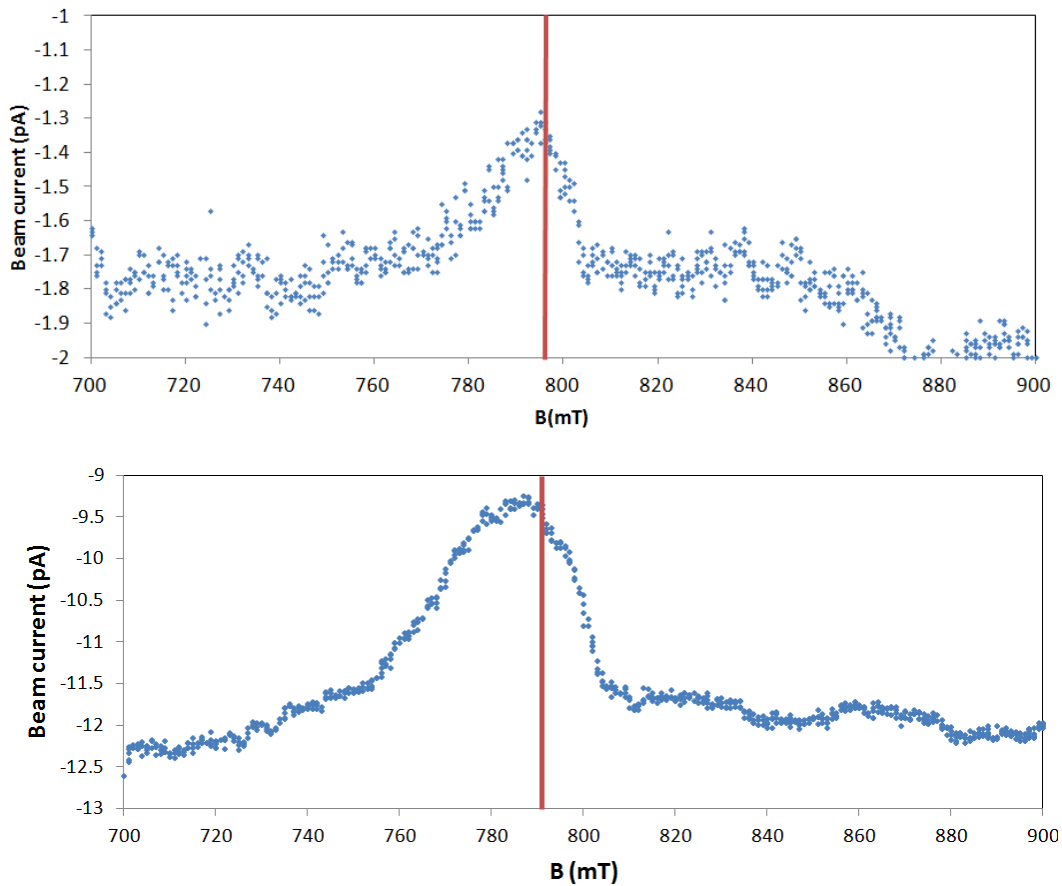


Figure 33. Beam current at 12.13 MHz. This is the highest energy run to date. The top scan was obtained at a lower dee voltage (220 mV_{pp} on the function generator) than the one beneath it (440 mV_{pp}). The vertical red line corresponds the theoretical location of H^+ resonance of 796 mT at a maximum energy of 157 keV. It is thought that the 9V battery is causing negative currents to be read.

The frequency has been tuned upward several times. At present, the highest RF frequency achieved is 12.13 MHz. At this frequency, the H^+ resonance should be at 796 mT, corresponding to a maximum energy of 157 keV. Two runs were performed with hydrogen, one at a lower dee voltage ($FG=220 \text{ mV}_{pp}$) and another at higher dee voltage ($FG=440 \text{ mV}_{pp}$). The high voltage probe seemed to be malfunctioning so the corresponding value of the dee voltages could not be accurately measured. Figure 30 shows the beam current as a function of magnetic field around the expected H^+ resonance for the two data runs. In the near future the cyclotron will be operated at even higher frequencies, hopefully culminating in the eventual maximum energy possible given the present magnetic field strength achievable.

4.7 Effect of Secondary Electrons

When ions collide with the current collector, they can cause electrons to be ejected. This results in an additional current to that caused by the ion beam itself. To prevent the loss of these secondary electrons, a 9 V bias was placed on the current collector. The effect of this modification on measured beam current was studied by performing two magnet scans- the first without the 9 V battery and the second with the bias voltage. The scans were performed at $f=3.67 \text{ MHz}$ and 2000 V_{pp} dee voltages using hydrogen and helium. The results are shown in Figure 31.

The beam current measured was lower with the addition of the voltage bias to the beam collector than without. This indicates that the bias reduces the emission of secondary electrons, resulting in a more accurate measurement of the beam current.

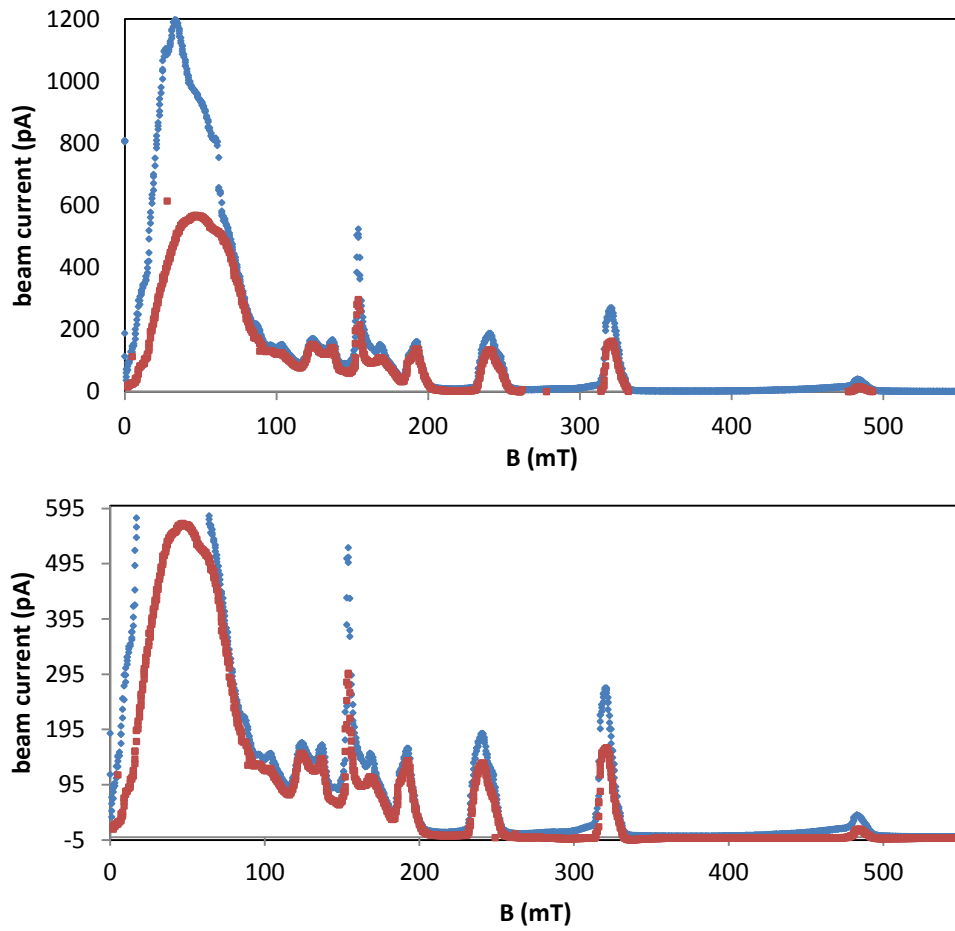


Figure 34. The effect of secondary electrons on measured currents. Two magnet scans were performed at $f=3.67$ MHz and $2000 V_{pp}$. The blue and red data points indicate the current without the bias and with a 9V bias, respectively. The beam current measured with the addition of a 9 V bias on the current collector indicates that the effect of secondary electron emission has been reduced.

Chapter 5

CONCLUSION & FUTURE WORK

The Houghton College cyclotron is currently functioning. The effect of varying operating parameters has been studied at low energies. Beam current as a function of dee voltage, filament float bias, current collector radius, and pressure has been measured. This data will be used in the future as an aide to maximize beam current. Furthermore, the RF frequency is being incrementally increased in the hope of attaining resonance at the maximum B-field, which will yield protons of 335 keV, deuterons up to 167 keV and singly ionized helium with 84 keV of energy. With a 70 A magnet power supply, proton energies up to 400 keV could be obtained.

In addition to increasing the proton energy, another immediate goal is to increase the beam current to the target. To this end, a Poisson Superfish and Simion model following the work of Koeth [26] is being adapted to simulate the effects of magnetic field shaping on the accelerated ions. These models will help determine the shape and thickness of ferromagnetic shims required to maximize magnetic focusing of the ion beam.

Once the magnetic field has been properly shaped and a 70 A magnet power supply has been purchased the cyclotron could be used in several low-energy nuclear physics experiments.

Two of reactions that could be measured are the (p, γ) resonances of ^{19}F and ^{31}P . In the first reaction $^{19}\text{F}(p, \gamma)^{16}\text{O}$ a proton reacts with a fluorine nucleus, resulting in an alpha particle, a gamma ray, and a residual oxygen nucleus. At certain proton energies, known as resonances, this reaction has a higher cross section. As can be seen in Figure 35, the ^{19}F reaction has resonances at proton incident energies of 225, 230, and 340.4 keV with total cross sections of 0.173, 0.041, and 82-104 mb, respectively [27]

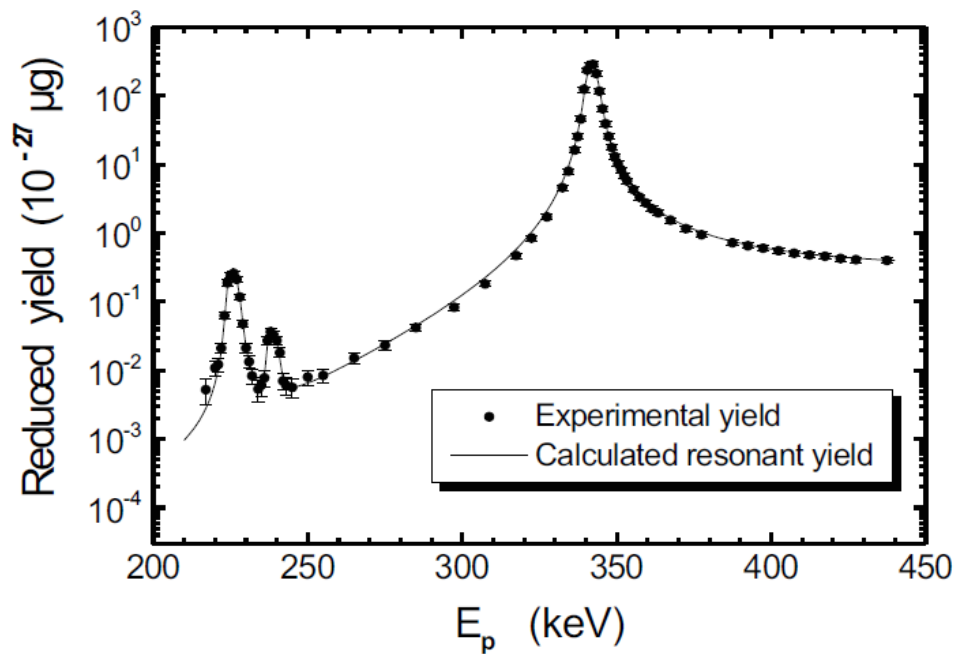


Figure 35. A cross section plot of the $^{19}\text{F}(p, \gamma)^{16}\text{O}$ resonance as a function of incident proton energy. The reduced yield is simply the cross section (in mb) times the thickness of the fluorine target in $\mu\text{g}/\text{cm}^2$. The highest yield resonance within operation limits of the Houghton College cyclotron occurs at an incident proton energy of 340.4 keV. Figure taken from Ref. [25].

The 340.4 keV high-yield resonance would be within the operating parameters of the Houghton College cyclotron. A target made of Teflon (which contains fluorine) could be placed in the cyclotron chamber. The gamma ray from the reaction would pass through the chamber wall and could be detected outside the chamber to indicate an event.

Another possible reaction is the $^2\text{H}(d,n)^3\text{He}$ d-d fusion reaction. A deuteron collides with deuterated polymer foil and fuses to form a helium nucleus, releasing a neutron with energies up to 2.45 MeV for incident deuterons of energies achievable with the Houghton college cyclotron. These would pass through the chamber wall to be used in low energy nuclear physics experiments.

In a second reaction, ${}^2\text{H}({}^3\text{He},\text{p}){}^4\text{He}$, ${}^3\text{He}$ ions would be accelerated and collide with a deuterated target or deuterons could be accelerated into a foil impregnated with ${}^3\text{He}$ and a reaction would occur releasing an 18 MeV proton. In order to allow these to exit the chamber, the target would have to have a line of sight to a detector mounted on one of the chamber ports so that the proton could pass through and be detected, as shown in Figure 36.

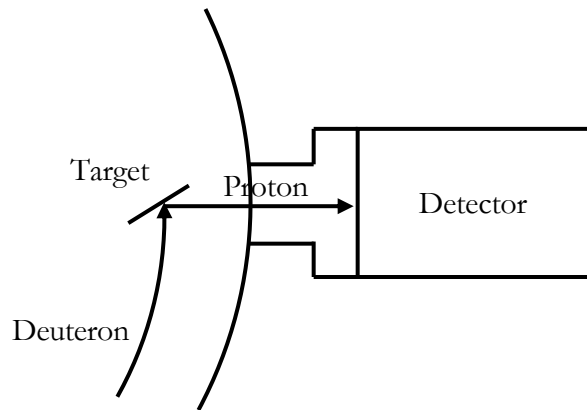
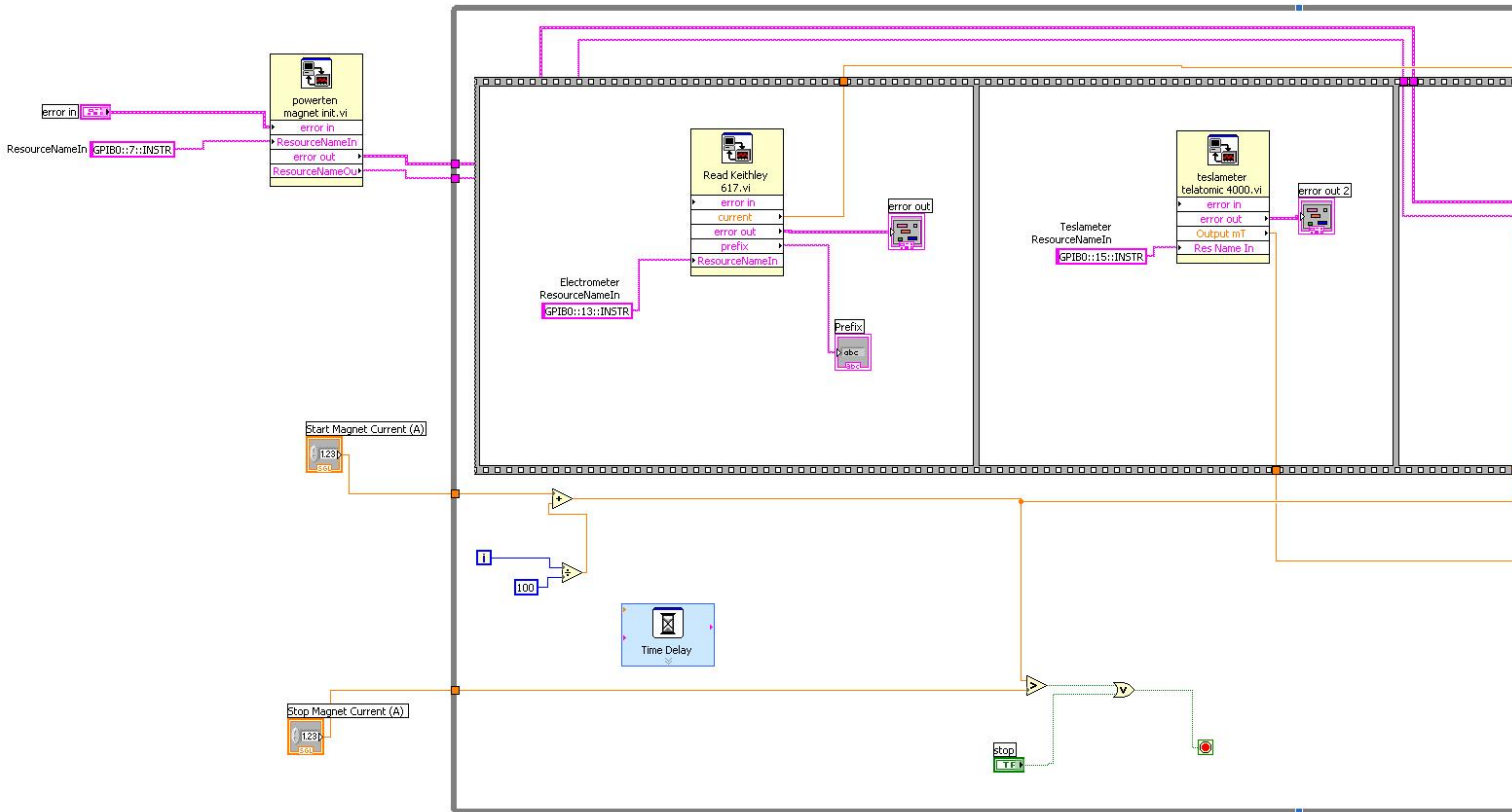


Figure 36. A schematic of an experiment measuring the ${}^2\text{H}({}^3\text{He},\text{p}){}^4\text{He}$ reaction. Here, an incident deuteron collides with a thin target impregnated with ${}^3\text{He}$, releasing a proton that can be detected.

With the potential to produce high energy neutrons or protons as well as detectable (p,γ) resonances, the Houghton College cyclotron can be used as an educational tool for studying low-energy nuclear physics reactions.

Appendix

This section contains the LabVIEW block diagram for the cyclotron magnet scan program, which allows the user to set a starting and ending magnet supply current and the program will increment the magnet supply and record the magnetic field strength as well as the beam current and output the results to a spreadsheet for analysis.



References

-
- [1] E. Rutherford, Proc. Royal Soc. (*London*). **117**, 300 (1927).
 - [2] R.J. Van de Graaff, Phys. Rev., **38**, 1919 (1931).
 - [3] R.J. Van de Graaff *et. al.*, Repts. Prog. in Phys. **11**, 1 (1948).
 - [4] R.J. Van de Graaff, Nucl. Instr. And Methods **8**, 195 (1960).
 - [5] M.S. Livingston and J.P. Blewett, *Particle Accelerators* (McGraw-Hill Book Company, New York 1962).
 - [6] E.O. Lawrence, *The evolution of the cyclotron*. Nobel Lecture, 1951.
 - [7] R. Wilderöe, *Archive elektrotechnische*. **21**, 387 (1928).
 - [8] M.S. Livingston, Ph.D. Thesis, University of California, Berkeley, 1931.
 - [9] E.O. Lawrence and M.S. Livingston, Phys. Rev. **40**, 19 (1932).
 - [10] E.O. Lawrence and D. Cooksey, Phys. Rev. **50**, 1131 (1936).
 - [11] E.O. Lawrence *et. al.*, Phys. Rev. **56**, 124 (1939).
 - [12] H.A. Bethe and M.E. Rose, Phys. Rev. **52**, 1254 (1937).
 - [13] J.R. Richardson *et.al.*, Phys. Rev. **69**, 669 (1946).
 - [14] A.G. Ingalls, *The Amateur Scientist*, September (1953).
 - [15] D.J. McGuire. *The Proceedings of the Iowa Academy of Science*. **68**, 474 (1961).
 - [16] J.C. Smith, undergraduate thesis, Knox College, Iowa, 2001.
 - [17] L. Dewan, undergraduate thesis, MIT, Massachusetts, 2007.
 - [18] F. Neil, Cyclotron Notes, 2002.
 - [19] P.V. Heuer *et. al.*, *Design of a 2 MeV Cyclotron*, 2009.
 - [20] J.J. Welch *et. al.*, *Advanced Accelerator Methods: The Cyclotron* (1987).
 - [21] T. Feder, *Physics Today* **57**, 30 (2004).
 - [22] Rutgers cyclotron
<http://www.physics.rutgers.edu/cyclotron/> (Author Unlisted).
 - [23] D. Haas, undergraduate thesis, Houghton College, New York, 2009.
 - [24] B.T. King, undergraduate thesis, Houghton College, New York, 2003.
 - [25] M.J. Cressman, undergraduate thesis, Houghton College, New York, 2006.
 - [26] T.W. Koeth, *Rutgers 12 Inch Cyclotron Ion Source Studies: Part1*, 2006 (Unpublished).
 - [27] K. Spyrou *et. al.*, Eur. Phys. J. A. **7**, 79 (2000).